

HIF-1 α regulates function and differentiation of myeloid-derived suppressor cells in the tumor microenvironment

Cesar A. Corzo,¹ Thomas Condamine,¹ Lily Lu,¹ Matthew J. Cotter,¹ Je-In Youn,¹ Pingyan Cheng,¹ Hyun-Il Cho,¹ Esteban Celis,^{1,2} David G. Quiceno,¹ Tapan Padhya,^{1,3} Thomas V. McCaffrey,^{1,3} Judith C. McCaffrey,^{1,3} and Dmitry I. Gabrilovich^{1,2}

¹H. Lee Moffitt Cancer Center and Research Institute, ²Department of Oncologic Sciences, and ³Department of Otolaryngology, University of South Florida, Tampa, FL 33612

Myeloid-derived suppressor cells (MDSCs) are a major component of the immune-suppressive network described in cancer and many other pathological conditions. We demonstrate that although MDSCs from peripheral lymphoid organs and the tumor site share similar phenotype and morphology, these cells display profound functional differences. MDSC from peripheral lymphoid organs suppressed antigen-specific CD8⁺ T cells but failed to inhibit nonspecific T cell function. In sharp contrast, tumor MDSC suppressed both antigen-specific and nonspecific T cell activity. The tumor microenvironment caused rapid and dramatic up-regulation of arginase I and inducible nitric oxide synthase in MDSC, which was accompanied by down-regulation of nicotinamide adenine dinucleotide phosphate-oxidase and reactive oxygen species in these cells. In contrast to MDSC from the spleen, MDSC from the tumor site rapidly differentiated into macrophages. Exposure of spleen MDSC to hypoxia resulted in the conversion of these cells to nonspecific suppressors and their preferential differentiation to macrophages. Hypoxia-inducible factor (HIF) 1 α was found to be primarily responsible for the observed effects of the tumor microenvironment on MDSC differentiation and function. Thus, hypoxia via HIF-1 α dramatically alters the function of MDSC in the tumor microenvironment and redirects their differentiation toward tumor-associated macrophages, hence providing a mechanistic link between different myeloid suppressive cells in the tumor microenvironment.

CORRESPONDENCE

Dmitry I. Gabrilovich:
dmitry.gabrilovich@moffitt.org

Abbreviations used: DCFDA, dichlorodihydrofluorescein diacetate; DFO, deferoxamine; HIF, hypoxia-inducible factor; HNC, head and neck cancer; IMC, immature myeloid cell; iNOS, inducible nitric oxide synthase; MDSC, myeloid-derived suppressor cell; NOX, nicotinamide adenine dinucleotide phosphate-oxidase; qRT-PCR, quantitative real-time PCR; ROS, reactive oxygen species; TAM, tumor-associated macrophage; TCCM, tumor cell conditioned medium.

Myeloid-derived suppressor cells (MDSCs) are one of the major components of the immune-suppressive network responsible for T cell defects in cancer. These cells also contribute to tumor progression via regulation of angiogenesis and tumor cell motility. MDSC is a large group of myeloid cells consisting of immature macrophages (M Φ), granulocytes, and DCs, as well as myeloid cells at earlier stages of differentiation (Sica and Bronte, 2007; Talmadge, 2007; Gabrilovich and Nagaraj, 2009; Peranzoni et al., 2010). In mice, MDSCs express both the myeloid lineage differentiation antigen Gr-1 (Ly6G and Ly6C) and α_M integrin CD11b. Two major groups of MDSCs are now identified: cells with granulocytic (CD11b⁺Ly6G⁺Ly6C^{low}) and monocytic (CD11b⁺Ly6G⁻Ly6C^{high}) phenotype (Movahedi et al., 2008; Youn et al., 2008).

In humans, MDSCs are generally defined as cells that express CD11b, the common myeloid marker CD33, but lack the expression of markers of mature myeloid and lymphoid cells and the MHC class II molecule HLA-DR (Almand et al., 2001; Zea et al., 2005; Diaz-Montero et al., 2009; Nagaraj et al., 2010). In tumor-free mice, MDSCs represent \sim 30% of the normal BM cells and $<$ 3% of all nucleated splenocytes. In tumor-bearing mice, this population undergoes dramatic expansion. In many tumor models the proportion of MDSC represents $>$ 20% of all splenocytes, and MDSCs are easily detectable in

© 2010 Corzo et al. This article is distributed under the terms of an Attribution-Noncommercial-Share Alike-No Mirror Sites license for the first six months after the publication date (see <http://www.rupress.org/terms>). After six months it is available under a Creative Commons License (Attribution-Noncommercial-Share Alike 3.0 Unported license, as described at <http://creativecommons.org/licenses/by-nc-sa/3.0/>).

tumors and lymph nodes (Kusmartsev and Gabrilovich, 2006; Rabinovich et al., 2007; Sica and Bronte, 2007; Gabrilovich and Nagaraj, 2009). Similar expansion, albeit to a lesser degree, is observed in patients with cancer. In the presence of appropriate cytokines in vitro and after adoptive transfer in vivo, MDSC can differentiate into mature myeloid cells (Kusmartsev and Gabrilovich, 2003). This differentiation is blocked, however, in the presence of tumor cell-conditioned media or in tumor-bearing hosts (Kusmartsev and Gabrilovich, 2003; Talmadge, 2007).

Extensive studies in recent years suggested several mechanisms of MDSC-mediated immune suppression that involve arginine (Bronte and Zanovello, 2005; Rodríguez and Ochoa, 2008) and cysteine (Srivastava et al., 2010) metabolism, expression of some surface molecules (Pan et al., 2010), up-regulation of reactive oxygen species (ROS), and production of different cytokines (Talmadge, 2007; Gabrilovich and Nagaraj, 2009). Practically all these studies were performed with MDSC isolated from peripheral lymphoid organs (mostly spleen).

Although an important role of MDSC in tumor-associated immune suppression is well established in recent years, its nature remains unclear. One of the major unresolved questions is the role of MDSCs in peripheral lymphoid organs and tumor tissues as well as their relationship with MΦ and DCs. The main paradox is that, despite the presence of a large number of MDSCs in spleens and lymph nodes of tumor-bearing mice and in the peripheral blood of cancer patients with advanced disease, T cells mostly retain the ability to respond to different tumor-nonspecific stimuli including viruses, lectins, costimulatory molecules, IL-2, and stimulation with CD3- and CD28-specific antibodies (Fricke et al., 2007; Monu and Frey, 2007; Nagaraj et al., 2007). In a sharp contrast, T cells directly isolated from tumors display profound defects in their ability to respond to those stimuli (Rabinovich et al., 1996; Lopez et al., 1998; Reichert et al., 2002). Some evidence may suggest that MDSC-mediated immune suppression in peripheral lymphoid organs could be mainly tumor antigen specific. MDSCs mediate antigen-specific T cell tolerance by taking up soluble antigens, including tumor-associated antigens, processing them, and presenting them to CD8⁺ T cells in the context of MHC class I (Kusmartsev et al., 2005; Movahedi et al., 2008).

The role of tumor-associated MDSC remains largely obscure. Despite the fact that the cells with the phenotype of MDSC are abundantly present in tumor tissues but are often referred to as monocytes, MΦ, or granulocytes, the relationship (or lack thereof) between MDSC and tumor-associated macrophages (TAMs) is unclear. This confusion is derived from the difficulties in clearly defining the phenotype of myeloid cells in the tumor site. This creates a convoluted, rather incoherent picture of the various functions of different myeloid cell subsets within the tumor. Ambiguity of the biological role of and the relationship between different myeloid cell populations within the tumor site severely limits our understanding of the biology of tumor progression and the development of targeted therapeutics.

In this study, we addressed this issue by investigating the function and differentiation of MDSC at the tumor site using an experimental model where tumors were generated as ascites. This allowed for a rapid isolation of cells and enabled direct experiments with adoptive transfer of MDSC directly into the tumor microenvironment. In this paper, we report that MDSCs in tumor-bearing mice display a biological dichotomy regulated by the tumor microenvironment. In peripheral lymphoid organs, MDSC primarily caused antigen-specific T cell nonresponsiveness, which was mediated by ROS. In contrast, within tumor microenvironment, MDSC with the same phenotype and morphology had low ROS levels but dramatically up-regulated NO production and arginase activity, which caused suppression of antigen-nonspecific T cell functions. In contrast to MDSC from the spleen, MDSC in the tumor microenvironment rapidly differentiated primarily into TAM. This process was mediated primarily by hypoxia via hypoxia-inducible factor (HIF) 1α. Our data thus help to explain the differences in the nature of T cell suppression between tumor and peripheral lymphoid organs in tumor-bearing hosts and suggest a regulatory pathway of myeloid cell function in the tumor microenvironment.

RESULTS

Phenotype and function of MDSC in the tumor site

To directly compare MDSC from the tumor site to MDSC from peripheral lymphoid organs (spleen), we have developed a model where EL-4 tumor grows as an ascites in C57BL/6 mice. The dose of EL-4 cells was selected to form an ascites within 3 wk after tumor injection. MDSCs in mice are broadly defined as Gr-1⁺CD11b⁺ cells. These markers were used to sort MDSC from within the spleen and tumor of the same mouse (Fig. 1 A). MDSC from both sites expressed the same level of Gr-1 and CD11b molecules and had similar mixed granulocytic and monocytic cell morphology (Fig. 1 B). Granulocytic MDSCs (CD11b⁺Ly6G⁺Ly6C^{low}) were a predominant type of MDSC in both sites. There was no difference between the ratio of granulocytic and monocytic (CD11b⁺Ly6G⁺Ly6C^{high}) MDSC isolated from tumor or spleens (Fig. 1 C). The CD11c marker specific for DCs was not expressed on either spleen or tumor MDSC, and <10% of MDSC expressed the CD115 or F4/80 markers of monocytes/macrophages (Fig. 1 C). Thus, MDSC from the tumor and spleen in this tumor model had similar morphology and phenotype.

To investigate whether these findings are confined to only an ascites model, we compared the phenotype of MDSC isolated from spleens and solid tumors in several models. EL-4 thymoma and B16.F10 melanoma were established as subcutaneous tumors, CC10 was a lung tumor spontaneously developed in transgenic mice. The *mCC10TA*g transgene was made by fusing the coding sequences of the SV40 TAG gene with the mCC10 promoter (Magdaleno et al., 1997). This promoter targets transgene expression specifically to proximal pulmonary lung epithelial Clara cells. These mice develop multifocal pulmonary adenocarcinoma in the lung at 3 mo of age. In all three models, tumor tissues and spleens

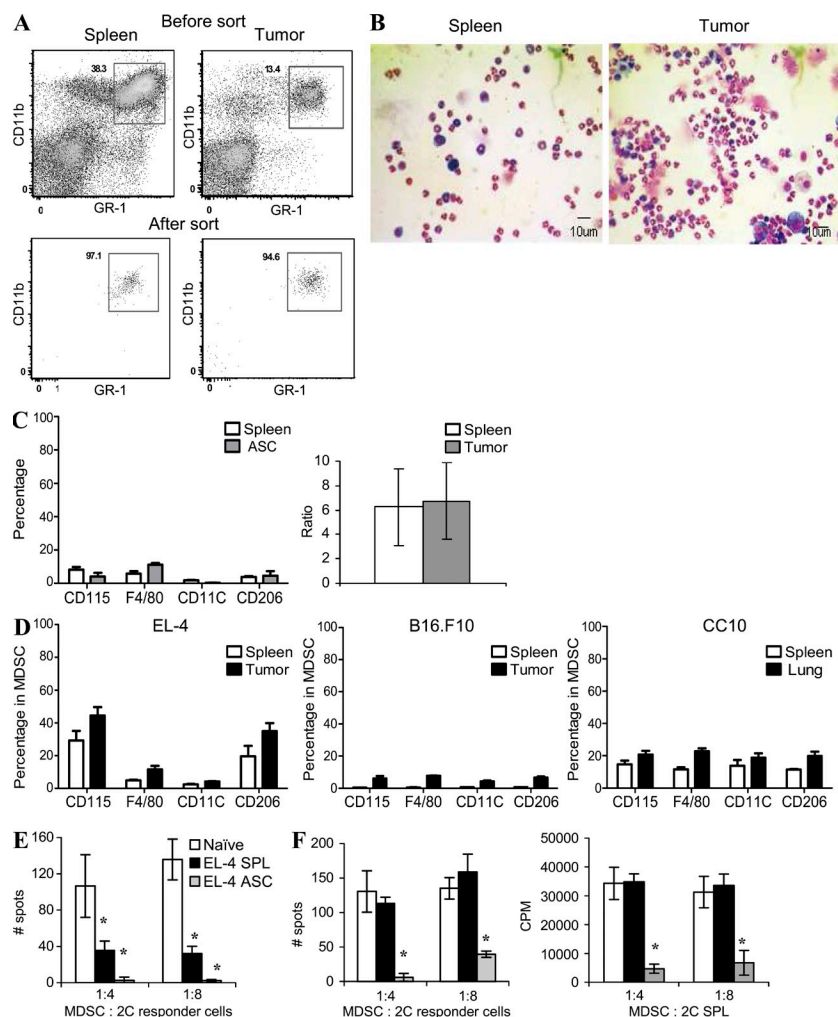


Figure 1. Phenotype and function of MDSC in tumor site. (A and B) 3×10^5 EL-4 tumor cells were injected i.p. into C57BL/6 mice. After 3 wk, spleens and cells from tumor ascites were collected. Gr-1⁺CD11b⁺ MDSC were sorted (A) and their morphology was evaluated by staining with H&E (B; 200 \times magnification). Bars, 10 μ m. (C, left) Surface markers in gated Gr-1⁺CD11b⁺ MDSC isolated from spleens and tumors of the same mice. (C, right) Ratio of granulocytic/monocytic MDSC. Five experiments were performed. Error bars show mean and SD. (D) Surface markers in gated Gr-1⁺CD11b⁺ MDSC isolated from spleens and solid tumors of the same mice. All tissues were subjected to the same enzymatic digestions. Three indicated tumor models were used. Each experiment included four mice. Mean \pm SD is shown. (E and F) Gr-1⁺CD11b⁺ cells purified from spleens of tumor-free mice (naive) or spleens (SPL) and ascites (ASC) of EL-4 tumor-bearing mice were cultured at indicated ratios with 10^5 splenocytes from transgenic 2C mice. (E) Splenocytes were stimulated with control and specific peptides. IFN- γ production was measured in quadruplicates in ELISPOT assay. Number of spots per 10^5 2C splenocytes is shown. Values in cells stimulated with control peptide were subtracted. *, statistically significant ($P < 0.05$) difference from naive mice. A typical example of four independent experiments is shown. (F) Splenocytes were stimulated with anti-CD3/CD28 antibodies. In addition to the measurement of IFN- γ production, evaluation of splenocyte proliferation was performed using 3 H-thymidine uptake. CPM, counts per minute. Thymidine uptake in cells stimulated with control peptide was $<1,000$ cpm. All experiments were performed in triplicates. A typical result of three performed experiments is shown. Error bars show mean and SD. *, statistically significant ($P < 0.05$) differences from naive mice.

were digested and the phenotype of MDSC was compared side by side. Tumor and spleen MDSC displayed a similar phenotype in all models. The proportion of F4/80⁺ cells was slightly higher in tumor-associated MDSC than in spleen MDSC. However, the differences were not statistically significant ($P > 0.05$; Fig. 1 D).

We compared the ability of tumor and spleen MDSC to suppress antigen-specific and -nonspecific T cell responses. Two basic functions of T cells were evaluated: IFN- γ production and T cell proliferation. The antigen-specific response to MHC class I-restricted SIYRYGL (SIY) peptide was measured in 2C transgenic CD8⁺ T cells. The antigen-nonspecific T cell response was evaluated after stimulation with anti-CD3/CD28 antibodies. MDSCs were isolated from the ascites and spleens of the same mice and were used under the same experimental conditions. Gr-1⁺CD11b⁺ immature myeloid cells (IMCs) from spleens of naive tumor-free mice were used as a control. As was demonstrated in previous studies, IMCs lack immunosuppressive activity (Kusmartsev et al., 2004, 2005; Zhou et al., 2007; Yamamoto et al., 2008). Both spleen and tumor MDSCs effectively suppressed the antigen-specific T cell response, although the level

of suppression was significantly ($P < 0.05$) higher in tumor MDSC (Fig. 1 E). However, the major differences were observed during the analysis of T cell response to nonspecific stimuli. Spleen MDSC did not suppress nonspecific T cell responses. In contrast, tumor MDSC exerted a profound suppressive effect (Fig. 1 F).

To evaluate MDSC function in the CC10 transgenic model of lung cancer, MDSCs were isolated from tumor or spleens of the 3-mo-old mice and then added to responder cells from naive mice stimulated with anti-CD3/CD28 antibodies. Tumor MDSC showed a marked suppressive activity, whereas spleen MDSC failed to suppress nonspecific T cell proliferation (Fig. S1 A). To assess antigen-specific T cell responses, we used OT-1 transgenic T cells expressing TCR specific for the OVA-derived epitope SIINFEKL. Tumor MDSC suppressed T cell proliferation in response to specific peptide at ratios as low as 1:8 (Fig. S1 B).

Our data show that MDSCs from the tumor site and spleen of the same mouse differ profoundly in the ability to suppress T cell function. Several factors have been previously implicated in suppressive activity mediated by MDSC. They include ROS, arginase, inducible nitric oxide synthase (iNOS),

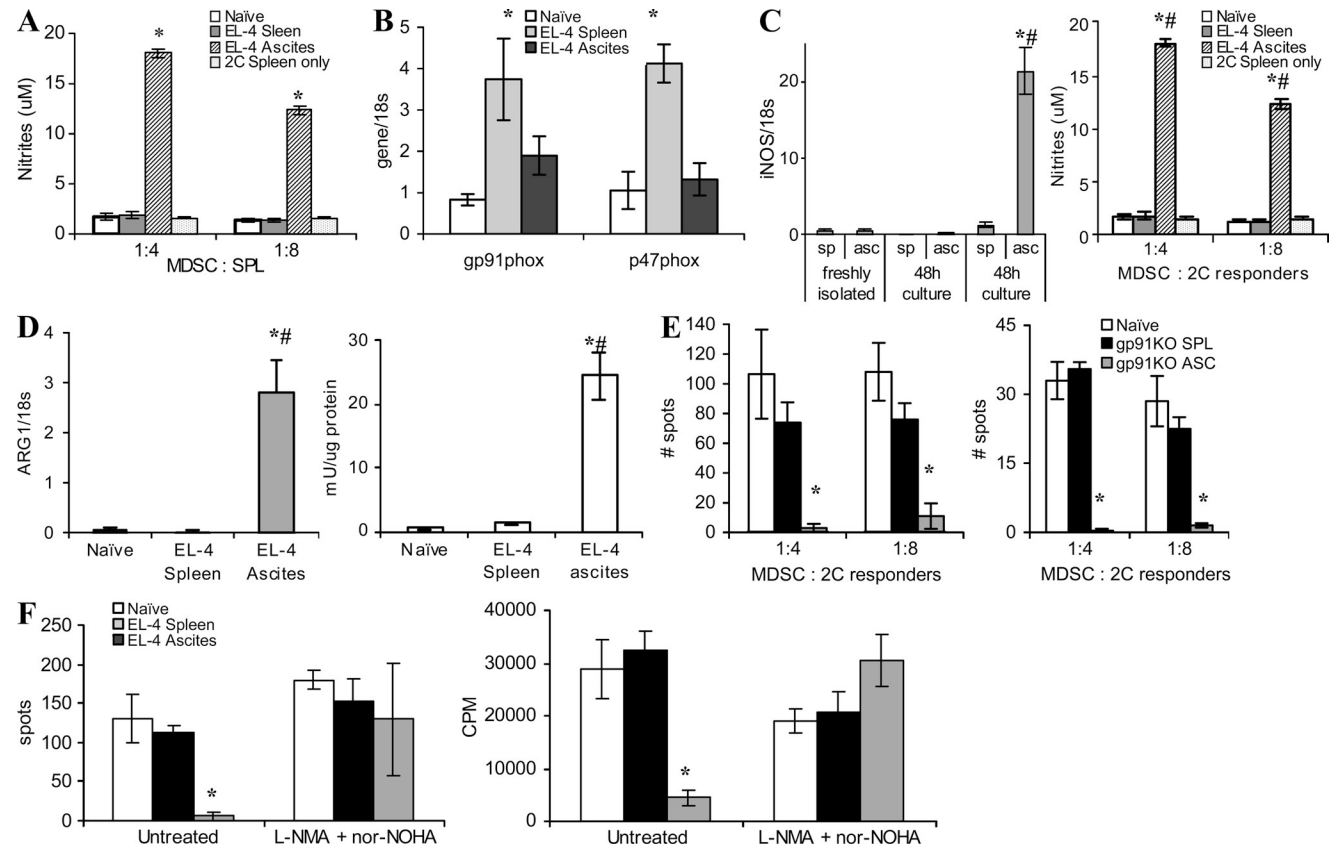


Figure 2. Factors regulating MDSC suppressive activity. (A) Cells collected from the tumor site or spleens of EL-4 tumor-bearing mice were stimulated with PMA, labeled with 1 μ M dichlorodihydrofluorescein diacetate (DCFDA), and stained with APC-conjugated anti-Gr-1 antibody and PerCP-conjugated anti-CD11b antibody. DCFDA fluorescence was measured in Gr-1⁺CD11b⁺ population by flow cytometry. Cumulative results from four independently performed experiments are shown. In all panels, * denotes statistically significant difference ($P < 0.05$) from naive mice. (B) RNA was extracted from Gr-1⁺CD11b⁺ cells isolated from spleens or tumor of the same mice and expression of *gp91^{phox}* and *p47^{phox}* was measured in quantitative real-time PCR (qRT-PCR). The experiment was performed in triplicates and repeated twice with the same result. (C) MDSCs from spleen and tumor ascites were stimulated with 30 ng/ml IFN- γ for 48 h and expression of *inos* was measured in qRT-PCR (left). The same cells were mixed at the indicated ratio with 2×10^5 splenocytes stimulated with anti-CD3/CD28 antibodies. After a 48-h incubation, culture medium was collected and assayed for nitrites (right). Experiments were performed in triplicates and repeated three times with the same results. #, statistically significant ($P < 0.05$) differences between MDSC isolated from spleen and tumor at the same time point. (D) Arginase 1 gene expression (left) and enzymatic activity (right) were evaluated in MDSC from tumor site and spleen. All experiments were performed in triplicates and repeated three times with the same results. *, statistically significant differences ($P < 0.05$) from naive mice; #, statistically significant ($P < 0.05$) differences between ascites and spleen of the same mice. (E) Suppressive activity of MDSC from gp91^{phox} knockout mice on IFN- γ production by transgenic 2C T cells after stimulation with either specific peptide (left) or anti-CD3/CD28 antibodies (right). Each experiment was performed in triplicates. Two experiments with the same results were performed. *, statistically significant differences ($P < 0.05$) from naive mice. (F) MDSCs isolated from spleens or tumor site were incubated at a 1:4 ratio with naive syngeneic splenocytes stimulated with anti-CD3/CD28 antibodies in the presence of iNOS (0.5 mM L-NNMA) and arginase (0.5 mM nor-NOHA) inhibitors. IFN- γ production was measured in ELISPOT assay and cell proliferation by incorporation of ³H-thymidine. Three experiments with the same results were performed. Error bars show mean and SD.

and NO (Gabrilovich and Nagaraj, 2009; Ostrand-Rosenberg and Sinha, 2009). We evaluated ROS levels within the population of MDSC from spleen and tumors. IMCs from spleen of naive mice served as controls. As expected, MDSC from spleens of tumor-bearing mice displayed a significantly higher level of ROS than the cells from tumor-free mice. Surprisingly, ROS production in tumor MDSC was significantly lower than that of spleen MDSC (Fig. 2 A). Expression of *gp91^{phox}* and *p47^{phox}* components of the nicotinamide adenine dinucleotide phosphate-oxidase (NOX) complex responsible for ROS production in MDSC (Corzo et al., 2009) was

significantly lower in MDSC from the tumor than that in MDSC from the spleen (Fig. 2 B).

In contrast, MDSC isolated from the tumor site had a much higher level of *inos* expression and NO production, as well as *arginase-1* expression and arginase activity, than did spleen MDSC from the same mice (Fig. 2, C and D). To identify the link between MDSC suppressive activity and ROS, we performed experiments with *gp91^{phox}* tumor-bearing mice. MDSCs from these mice do not produce ROS (Corzo et al., 2009). Lack of ROS did not affect the suppressive potential of tumor MDSC but completely eliminated the suppressive

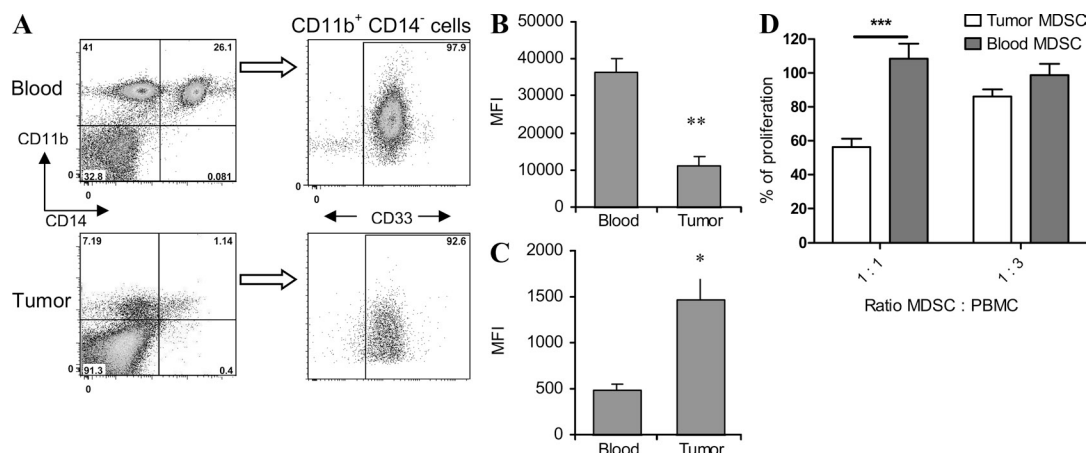


Figure 3. MDSC in peripheral blood and tumor tissues of cancer patients. (A–C) Peripheral blood and tumor tissues were collected from patients with HNC during surgical resection. Single cell suspensions were prepared as described in Materials and methods and cells were stained with anti-CD11b, anti-CD14, and anti-CD33 antibodies. (A) A typical example of gating of CD11b⁺CD14⁻CD33⁺ MDSC from the same patient in flow cytometry. (B) Cells were stained with DCFDA to detect ROS level within the population of CD11b⁺CD14⁻CD33⁺ cells from the same patient. Cumulative results from six patients are shown. **, statistically significant difference between MDSC in the tumor site and peripheral blood ($P = 0.007$). MFI, mean fluorescence intensity. (C) Cells were labeled with anti-iNOS antibody and the protein level was measured within the population of CD11b⁺CD14⁻CD33⁺ cells. Cumulative results from six patients are shown. *, statistically significant difference between MDSC in the tumor site and peripheral blood ($P = 0.04$). (D) Proliferation of PHA-stimulated mononuclear cells in the presence of MDSC isolated from tumor and peripheral blood of the same patient. PBMCs (10^5 /well) were stimulated with 5 μ g/ml PHA in the presence of indicated amount of MDSC. Proliferation was measured in triplicate on day 3 by uptake of ³H-thymidine. Proliferation of PBMC in the absence of MDSC was considered 100%. ***, statistically significant difference between groups ($P = 0.0008$). Samples from three patients were tested and cumulative results are shown. Error bars show mean and SD.

activity of spleen MDSC (Fig. 2 E). Inhibition of iNOS with LMMA and of arginase I with nor-NOH completely abrogated suppressive activity of tumor-derived MDSC (Fig. 2 F). Thus, MDSCs from the tumor use primarily arginase and NO to suppress T cell function, whereas splenic MDSCs use primarily ROS.

We asked whether up-regulation of iNOS and down-regulation of ROS also occurred in MDSC from solid tumors. To address this question we used s.c. EL-4 tumors. Amounts of iNOS and ROS level were measured within the Gr-1⁺CD11b⁺ population of tumor and spleen MDSC using flow cytometry immediately after enzymatic digestion of tissues. Tumor MDSC displayed substantially higher levels of iNOS than did spleen MDSC (Fig. S2). Conversely, the level of ROS, as well as the expression of *p47^{phox}* and *gp91^{phox}* subunits of NOX, in tumor MDSC was substantially lower than in spleen MDSC (Fig. S3).

Our data indicate that MDSC from the tumor site and peripheral lymphoid organs of tumor-bearing mice differ in their ability to produce ROS and NO. To test whether a similar phenomenon is observed in cancer patients, we studied paired samples of peripheral blood and tumor tissues obtained from patients with head and neck cancer (HNC). MDSCs were defined as CD14⁺CD11b⁺CD33⁺ cells (Fig. 3 A). Previous studies have shown that these cells have the functional characteristics of MDSC (Zea et al., 2005; Nagaraj et al., 2010). ROS and iNOS were measured in MDSC using flow cytometry. MDSC in the tumor had significantly lower ROS production than did MDSC in peripheral blood (Fig. 3 B).

In contrast, iNOS levels in tumor MDSC were substantially higher than in blood MDSC (Fig. 3 C). To evaluate functional activity, MDSCs were sorted from peripheral blood and tumor tissues. To account for the possible effect of enzymes used for tissue digestion on MDSC function, peripheral blood was treated the same way as tumor tissues. MDSCs were then added to patients' mononuclear cells, and T cell proliferation in response to PHA was measured. MDSC isolated from peripheral blood did not affect PHA-inducible T cell proliferation, whereas MDSC from tumor tissues significantly ($P = 0.0008$) decreased it (Fig. 3 D). Thus, these results, which are similar to those observed in tumor-bearing mice, suggest that differences in MDSC function may represent a general phenomenon.

Effect of the tumor microenvironment on MDSC function and differentiation

MDSCs are a heterogeneous group of cells. Therefore, despite similarities in the morphology and phenotype of MDSC isolated from tumor sites and spleens, it is difficult to formally exclude the possibility that MDSC in different sites may represent different populations of myeloid cells. To address this question, as well as to identify the mechanisms of MDSC function in the tumor site, we used a direct transfer of Gr-1⁺CD11b⁺ MDSC isolated from spleens of EL-4 tumor-bearing congenic (CD45.1⁺) mice into the ascites of EL-4 tumor-bearing C57BL/6 (CD45.2⁺) recipients. EL-4 cells expressed the CD45.2 but not the CD45.1 marker (unpublished data). This allowed for discrimination between tumor

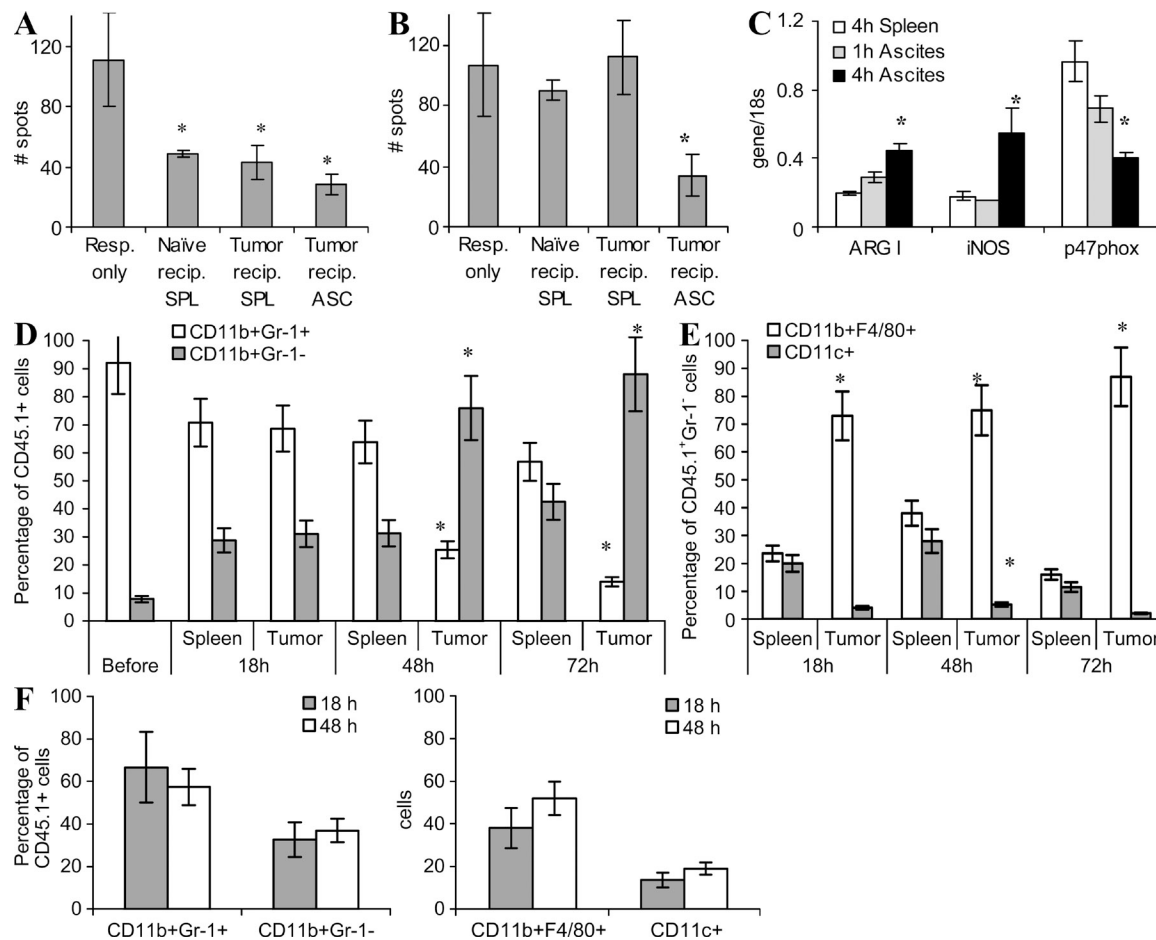


Figure 4. Effect of the tumor microenvironment on MDSC function and differentiation. MDSC isolated from spleens of congenic CD45.1⁺ mice bearing 3 wk s.c. EL-4 tumors were transferred into ascites of CD45.2⁺ EL-4 tumor-bearing recipients. CD45.1⁺ donor cells were recovered using magnetic beads 4 h after cell transfer. For controls, CD45.1⁺ MDSC were transferred i.v. into EL-4 tumor-bearing recipients or naive recipients and recovered from spleens 4 h after cell transfer. (A) After adoptive transfer, CD45.1⁺ MDSCs were cultured with 2C spleen responder cells (Resp.; 1:4 ratio) stimulated with control and specific peptides. IFN- γ production was measured by ELISPOT assay. The number of spots per 10⁵ splenocytes is shown. Values in cells stimulated with control peptide were subtracted. Each experiment was performed in triplicates and repeated twice. *, statistically significant differences ($P < 0.05$) from the values in splenocytes cultured alone. Error bars show mean and SD. (B) Similar experiments performed using stimulation with anti-CD3/CD28 antibodies. Error bars show mean and SD. (C) Evaluation of gene expression of *arg1*, *iNOS*, and *p47^{phox}* in MDSC postadoptive transfer. Each experiment was performed in triplicates and repeated twice with the same results. Error bars show mean and SD. (D and E) Differentiation of MDSC at different time points after transfer. *, statistically significant ($P < 0.05$) differences between spleens and ascites. (D) The percentage of Gr-1⁺CD11b⁺ MDSC among all CD45.1⁺ donor cells. Before, the phenotype of MDSC before transfer to the mice. Error bars show mean and SD. (E) The percentage of mature macrophages (F4/80⁺CD11b⁺Gr-1⁻) and DCs (CD11c⁺CD11b⁺Gr-1⁻) among CD45.1⁺ donor cells. Mean \pm SD from three experiments is shown. In D and E, * denotes statistically significant ($P < 0.05$) differences between the proportion of cells in spleens and tumors at the same time point. (F) Differentiation of MDSC in tumor-free peritoneum. Congenic CD45.1⁺ mice were injected i.p. with 1 ml thioglycollate. 3 d later, 5×10^6 MDSCs isolated from spleen of EL-4 tumor-bearing C57BL/6 (CD45.2⁺) mice were injected i.p. Cells were collected 18 h after the injection and the proportion of different myeloid cells was measured within the gated population of CD45.2⁺ donor cells by flow cytometry. Two independent experiments were performed. Error bars show mean and SD.

cells and MDSC. In parallel, MDSCs were injected i.v. into either EL-4 tumor-bearing or tumor-free recipients to evaluate donor cells in the spleen. Donor cells isolated from spleens 4 h after the transfer significantly ($P < 0.01$) suppressed antigen-specific T cell responses (Fig. 4 A). However, these cells failed to inhibit the nonspecific T cell response (Fig. 4 B). In contrast, donor cells isolated from tumor site 4 h after the transfer exhibited strong suppressive activity of both antigen-specific and nonspecific T cell functions (Fig. 4, A and B).

Expression of *arg1* and *inos* was significantly higher, whereas expression of *p47^{phox}* was significantly lower, in donor cells isolated from tumor than in those from spleens (Fig. 4 C). Dramatic suppressive activity, as well as high levels of *arg1* and *inos* and down-regulation of ROS, was observed in donor cells isolated from tumor sites 18 h after the transfer (Fig. S4). Thus, substantial changes in MDSC suppressive activity and up-regulation of *inos* and *arg1* were observed as early as 4 h after adoptive transfer of MDSC into the tumor site.

It is known that MDSC can differentiate into mature myeloid cells. We therefore investigated the fate of these cells after transfer into the tumor site. CD45.1⁺ MDSCs isolated from spleens of tumor-bearing mice were transferred i.v. or injected directly into ascites of CD45.2⁺ recipients. No differences were observed in the phenotype of cells isolated 4 h after the transfer (unpublished data). 18 h after the transfer, most of the donor MDSC (>70%) in the spleen and tumor site still retained the MDSC phenotype (Gr-1⁺CD11b⁺; Fig. 4 D and Fig. S4). Those donor cells that lost Gr-1 expression were represented in the spleens evenly by CD11c⁺ DCs and CD11b⁺F4/80⁺ MΦ (Fig. 4 E). In sharp contrast, most of the Gr-1[−] donor cells in tumor site were CD11b⁺F4/80⁺ MΦ (Fig. 4 E and Fig. S5). After 48 h, the proportion of Gr-1⁺CD11b⁺ MDSC among donor cells in spleens remained about the same (>60%). However, in the tumor site it was substantially decreased to <30% of all donor cells (Fig. 4 D). After 48 h, practically all Gr-1[−] donor cells in the tumor site, but only 30% of cells in the spleen, were F4/80⁺CD11b⁺ MΦ. In contrast, few Gr-1[−] cells in the tumor site express the CD11c marker of DCs, whereas in spleen >30% of these cells were CD11c⁺ (Fig. 4 E). 3 d after the transfer, all Gr-1[−] donor cells in the tumor site remained F4/80⁺CD11b⁺ MΦ, whereas MΦ represented <20% of these cells in spleen (Fig. 4 E).

Because tumors in this model were established in peritoneum, we investigated the possible effect of a tumor-free peritoneum microenvironment on MDSC differentiation using CD45.1⁺ congenic recipients. To retain MDSC in peritoneum cavity, thioglycollate was injected i.p. 3 d before injection of MDSC. Donor cells rapidly migrated out from peritoneum cavity even in the presence of thioglycollate; therefore, the analysis was possible only during the first 48 h after the transfer. The proportion of donor cells retaining MDSC phenotype (Gr-1⁺CD11b⁺) 2 d after the transfer was ~60%, which was substantially higher than the proportion of these cells in tumor site (Fig. 4, D and F). CD11b⁺F4/80⁺ MΦ represented <50% of Gr-1[−] donor cells 48 h after the transfer of MDSC. This was substantially lower than the proportion of these cells found in tumor (Fig. 4, E and F). Thus, the pattern of MDSC differentiation in peritoneum in tumor-free mice was very different from that observed in the ascites of tumor-bearing mice. It suggests that the effect of tumor ascites on MDSC differentiation was mediated primarily by tumor itself rather than peritoneum microenvironment. Thus, in the tumor microenvironment, MDSC rapidly differentiated into F4/80⁺CD11b⁺ MΦ. In contrast, MDSC in spleens remained undifferentiated much longer and differentiated equally to MΦ and DCs.

Regulation of MDSC function by hypoxia

Our data demonstrates that the tumor microenvironment rapidly changes the function of MDSCs and promotes their differentiation to TAM. We investigated the possible mechanism of this effect. Hypoxia is one of the major characteristics of the tumor microenvironment. Therefore, we tested the effect of hypoxia on MDSC. MDSCs isolated from spleens of

tumor-bearing mice were incubated in complete culture medium and GM-CSF at normoxic or hypoxic (1% O₂) conditions for 48 h. Hypoxia significantly ($P < 0.05$) reduced the expression of *gp91^{phox}* and *p47^{phox}* components of NOX (Fig. 5 A), which resulted in a substantial decrease in the level of ROS production in these cells (Fig. 5 B). In contrast, hypoxia dramatically up-regulated expression of *arg1* and *inos* (Fig. 5 C). MDSC cultured in hypoxia acquired the ability to suppress T cell proliferation and IFN-γ production in response to nonspecific stimuli (anti-CD3/CD28 antibody; Fig. 5 D). This effect was independent of the presence of tumor cell-conditioned medium in the culture (Fig. 5 E). Thus, hypoxia recapitulated the effect of the tumor microenvironment on MDSC function.

To assess the effect of hypoxia on mouse MDSC differentiation, Gr-1⁺CD11b⁺ cells from spleens of tumor-bearing mice were cultured for 5 d in normoxia or hypoxia in the presence of GM-CSF. Hypoxia caused accumulation of cells with macrophage morphology (Fig. 5 F). After a 5-d culture under hypoxic conditions, the proportion of Gr-1⁺CD11b⁺ MDSC was fourfold lower compared with cells cultured at normoxia ($P < 0.01$), whereas the proportion of Gr-1[−]CD11b⁺F4/80⁺ MΦ was significantly higher ($P < 0.05$; Fig. 5 G and Fig. S6). In contrast, the proportion of CD11c⁺ cells was significantly ($P < 0.05$) higher among the cells cultured at normoxia than those incubated at hypoxia (Fig. 5 G). In addition, the majority of cells that differentiated from MDSC under hypoxia were positive for nonspecific esterase, the enzyme specific for monocytes/MΦ (Fig. 5 H). Thus, these data indicate that hypoxia promoted differentiation of MDSC to MΦ, which is similar to the effect observed in the tumor microenvironment.

Using the hypoxia-sensitive compound pimonidazole, we evaluated distribution of F4/80⁺ and Gr-1⁺ cells in more and less hypoxic areas of solid s.c. EL-4 tumor. More hypoxic areas of tumors contained significantly higher numbers of F4/80⁺ MΦ than less hypoxic areas ($P < 0.05$; Fig. 5, I and J). These results are consistent with previously reported observations about accumulation of TAM in hypoxic areas of tumor (Lewis and Murdoch, 2005; Movahedi et al., 2010). In contrast, the number of Gr-1⁺ cells in these areas was not different (Fig. 5, I and J).

We then asked whether hypoxia could cause functional polarization of MΦ cells during their differentiation from MDSC. MDSCs isolated from spleens of tumor-bearing mice were cultured at normoxia and hypoxia for 5 d, followed by isolation of F4/80⁺ cells and evaluation of their cytokine gene expression. As controls, we used F4/80⁺ MΦ obtained from peritoneal cavities on naive mice and F4/80⁺ cells collected from the ascites of tumor-bearing mice. As expected, TAM expressed substantially higher levels of *arg1* and *il-10* than control peritoneal MΦ (Fig. S7). MΦ generated from MDSC under normoxic conditions expressed *inos* and *il-6* but no or very little *il-12*, *il-10*, or *arg1*. In contrast, MΦ generated under hypoxic conditions expressed substantially higher levels of *il-10*, *arg1*, *iNOS*, *il-12*, and *il-6* (Fig. S7).

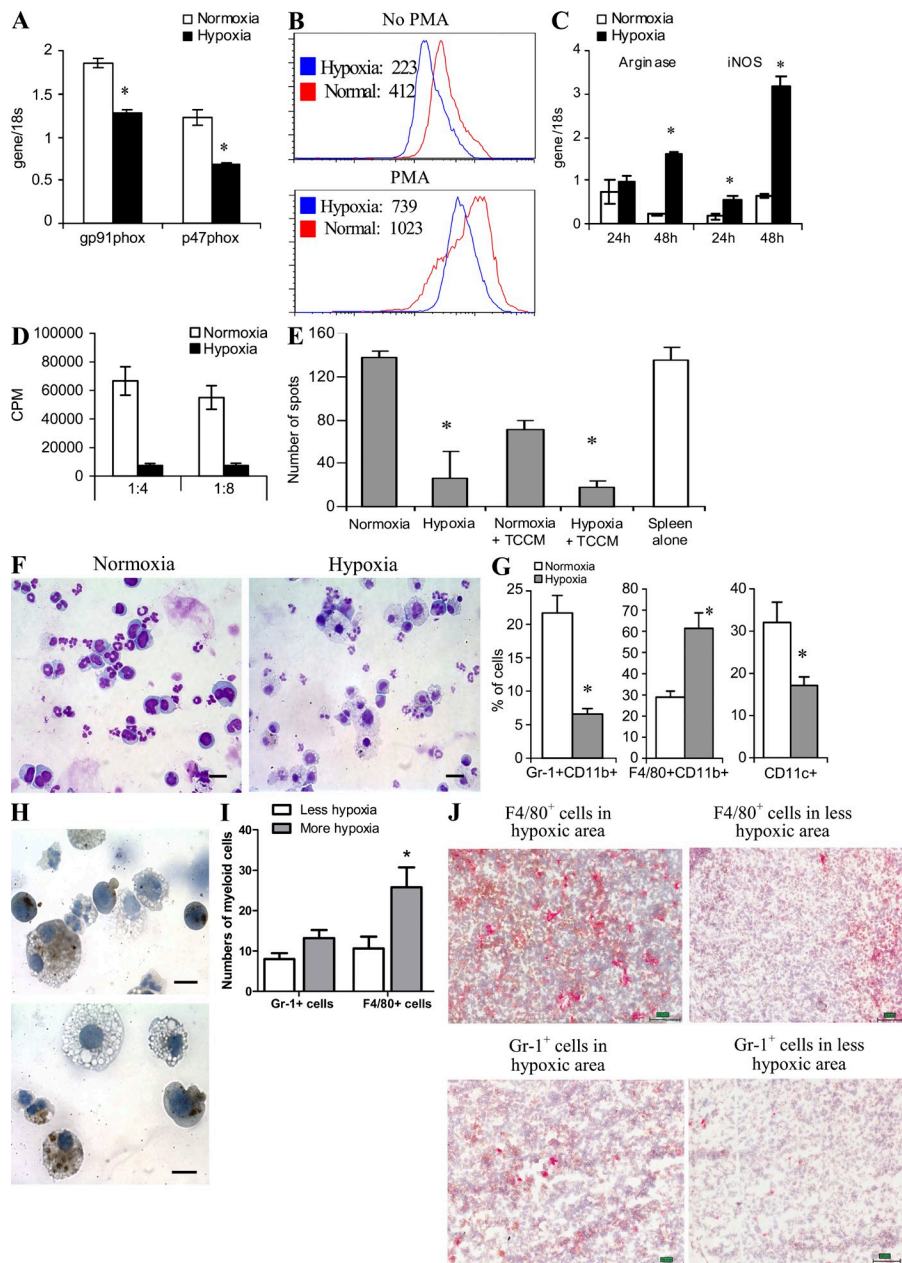


Figure 5. Regulation of MDSC function by hypoxia.

MDSCs were isolated from spleens of CT26 tumor-bearing mice and cultured in medium containing 10 ng/ml GM-CSF and 25% CT26 tumor cell conditioned medium (TCCM) under normoxic and hypoxic (1% O₂) conditions using a hypoxic chamber. (A) Expression of NOX subunits was evaluated in triplicates after 2 d of culture using qRT-PCR. Results are shown as mean \pm SD from three experiments performed with similar results. *, statistically significant ($P < 0.05$) differences between normoxia and hypoxia groups. (B) Cells were collected after 3 d of culture, loaded with DCFDA, and labeled with anti-Gr-1 and anti-CD11b antibodies. Fluorescence intensity of DCFDA was measured within the Gr-1⁺CD11b⁺ population. A typical result of three independently performed experiments is shown. (C) Expression of *argl* and *inos* was evaluated in triplicates in MDSC after 24- and 48-h incubations in hypoxic and normoxic conditions using qRT-PCR. Results from three independently performed experiments are shown. *, statistically significant ($P < 0.05$) differences between normoxia and hypoxia groups. (D) MDSCs were cultured for 48 h under normoxic or hypoxic conditions and their ability to suppress proliferation of anti-CD3/CD28-stimulated splenocytes was evaluated. Cell proliferation was measured in triplicates by ³H-thymidine uptake. A typical result from two performed experiments is shown. (E) BM cells were cultured for 3 d in media containing 10 ng/ml GM-CSF and 25% TCCM. After that time, cells were incubated under normoxic or hypoxic conditions for an additional 2 d. Gr-1⁺ cells were isolated and cultured with splenocytes from BALB/c mice stimulated with anti-CD3/CD28 antibodies. Production of IFN- γ was measured in triplicates by ELISPOT assay. *, statistically significant ($P < 0.05$) differences from values of splenocytes cultured alone. Two independent experiments were performed. (F) MDSCs were cultured for 5 d with 10 ng/ml GM-CSF and

25% TCCM in normoxia or hypoxia and then fixed and stained with H&E (400 \times magnification). Bars, 10 μ m. A typical example of two independently performed experiments is shown. (G) Phenotype of MDSC cultured for 5 d in hypoxia or normoxia. The proportions of cells with indicated phenotype were evaluated by flow cytometry. Cumulative results of four performed experiments are shown. *, statistical significant differences ($P < 0.05$) between the groups. Error bars in A, C-E, and G show mean and SD. (H) Cells derived from a 5-d culture of MDSC in hypoxia were tested for nonspecific esterase activity. Assay was repeated using cells isolated from two independent experiments. Bars, 10 μ m. (I and J) An association between the presence of M Φ and MDSC in hypoxic areas of the tumor. (I) Number of Gr-1⁺ or F4/80⁺ cells per one 800- μ m \times 600- μ m field. A total of 8–16 fields was counted for each area and results are shown as mean \pm SD. *, statistically significant ($P < 0.05$) differences between areas with less and more hypoxia. (J) Representative areas of s.c. EL-4 tumors are shown. Brown, staining with antibody detecting area of hypoxia; red; F4/80⁺ or Gr-1⁺ cells. Bars, 100 μ m.

HIF-1 α regulates MDSC differentiation and function

Up-regulation of HIF-1 α is one of the major effects of hypoxia. We investigated the possible role of HIF-1 α in the regulation of MDSC differentiation and function. A 4-h incubation of spleen MDSC under hypoxia resulted in substantial up-regulation of HIF-1 α (Fig. 6 A). To test the possible role of this transcription

factor on MDSC function, we used deferoxamine (DFO), which stabilizes HIF-1 α and serves as an HIF-1 α mimetic. Spleen MDSCs from tumor-bearing mice were treated with DFO for 48 h, washed, and then added to splenocytes stimulated with anti-CD3/CD28 antibodies. Nontreated MDSC did not suppress nonspecific T cell proliferation (Fig. 6 B) or

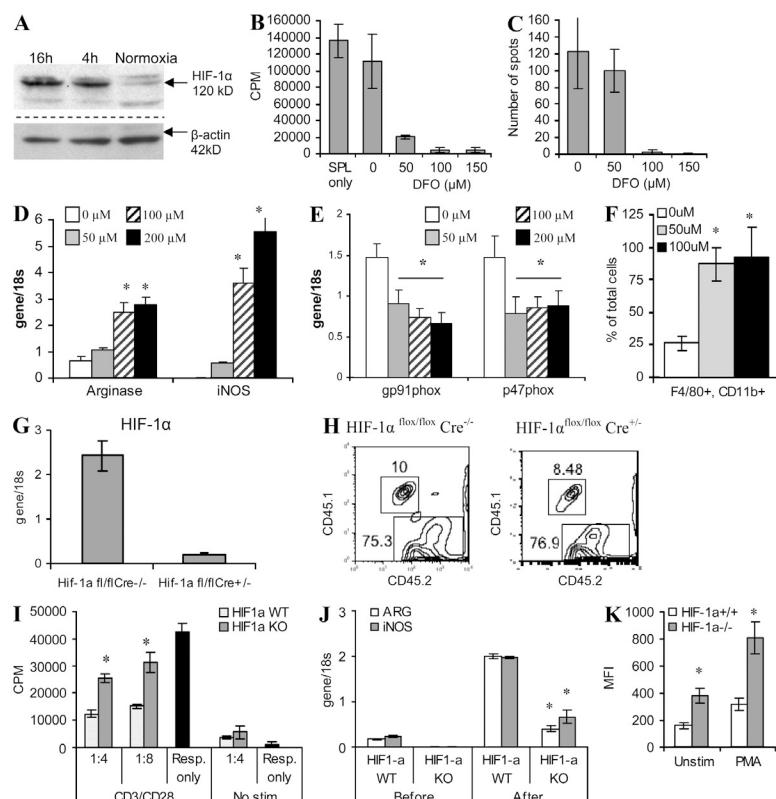


Figure 6. HIF-1α regulation of MDSC function. (A) MDSCs isolated from spleens of EL-4 tumor-bearing mice were cultured with 10 ng/ml GM-CSF in hypoxia for 4 or 16 h. The level of HIF1-α was measured by Western blotting. A typical example of three independently performed experiments is shown. (B–F) MDSCs were treated with various concentrations of HIF-1α stabilizer DFO in the presence of 10 ng/ml GM-CSF for 48 h and then washed and used in the experiments. No effect of DFO on MDSC cell viability was observed (not depicted). Each experiment was performed in triplicates and repeated two times with the same result. Results are shown as mean ± SD. (B and C) Effect of MDSC on proliferation (B) and IFN-γ production (C) of splenocytes stimulated with anti-CD3/CD28 antibodies. (D and E) Effect of a 48-h treatment of MDSC with DFO on the expression of *arg1*, *inos*, *gp91^{phox}*, and *p47^{phox}*. Each experiment was performed in triplicates. Three experiments were performed with the same result. (F) Percentage of F4/80⁺CD11b⁺ MΦ differentiated from MDSC treated with DFO for 5 d. Cumulative results (mean ± SD) of three experiments are shown. In D and F, * denotes statistically significant ($P < 0.05$) differences from untreated (0 μM) samples. (G) Evaluation of BM reconstitution by BM cells from HIF-1α-deficient mice. Expression is shown of *hif-1α* in HIF-1α^{fl/fl}Cre^{+/+} and HIF-1α^{fl/fl}Cre^{-/-} mice after treatment with poly I:C using real-time PCR. Experiments were performed in triplicates in three mice. Error bars show mean and SD. (H) Reconstitution of lethally irradiated CD45.1⁺ congenic mice with CD45.2⁺ BM from HIF-1α-deficient (HIF-1α^{fl/fl}Cre^{+/+}) or WT (HIF-1α^{fl/fl}Cre^{-/-}) mice. Blood of mice 2 wk after BM transfer was tested. (I–K) CD45.1⁺ lethally irradiated recipients were reconstituted with BM cells from HIF-1α knockout (KO) or WT CD45.2⁺ mice. 2 wk later, mice were inoculated s.c. with 5×10^5 EL-4 tumor cells. 3 wk after that, CD45.2⁺ HIF-1α WT or KO MDSC were isolated from spleens of tumor-bearing mice and then transferred into ascites of congenic CD45.1⁺ mice. 12 h later, CD45.2⁺ CD11b⁺ donor cells were isolated and used in the subsequent experiments. (I) The MDSCs were cultured with anti-CD3/CD28 antibody-activated T cells (Resp., responder cells) and their proliferation was measured by ³H-thymidine incorporation. Experiments were performed in triplicates. Mean ± SD is shown. Experiments were performed twice with the same result. (J) Expression of *arg1* and *inos* was analyzed in the MDSC before and after adoptive transfer into the tumor milieu. Two independent experiments were performed in triplicates. In J and K, * denotes statistically significant ($P < 0.05$) differences between the groups. Error bars show mean and SD. (K) ROS level in MDSC after the adoptive transfer was determined with DCFDA. Cumulative results of two experiments are shown. Error bars show mean and SD.

IFN-γ production (Fig. 6 C). However, MDSC pretreated with DFO caused profound suppression of T cell function (Fig. 6, B and C). DFO caused significant up-regulation of the expression of *arg1* and *inos* and a decrease in the expression of NOX components *p47^{phox}* and *gp91^{phox}* (Fig. 6, D and E). It also promoted MΦ differentiation from MDSC during a 5-d culture with GM-CSF (Fig. 6 F). Collectively, these results were very similar to the effect of hypoxia on MDSC and suggested that HIF-1α could be responsible for the observed effect of the tumor microenvironment on these cells.

To directly test this possibility, we used mice with conditional HIF-1α deletion. HIF-1α flox mice were crossed with Mx-Cre mice and HIF-1α deletion was induced by repeated poly:I:C administration (Fig. 6 G). Poly:I:C is a strong inducer of type I IFN and so would dramatically affect MDSC function. Therefore, to exclude this possibility and to make sure that HIF-1α deletion is confined only to hematopoietic cells, we used BM reconstitution of WT recipients. BM cells from CD45.2⁺ HIF-1α-deficient (HIF-1α^{fl/fl}Cre^{+/+}) or control (HIF-1α^{fl/fl}Cre^{-/-}) mice were used to reconstitute lethally irradiated CD45.1⁺ congenic naive mice. BM progenitors

from HIF-1α-deficient and WT mice showed similar engraftment potential (Fig. 6 H). 2 wk after BM transfer, mice were inoculated s.c. with EL-4 tumor cells. No significant differences in tumor growth between the groups were seen (unpublished data). Populations of myeloid cells were evaluated when the tumor reached 1.5 cm in diameter (3 wk after tumor injection). Gr-1⁺CD11b⁺ MDSC were expanded in spleens of tumor-bearing mice. To assess the effect of the tumor microenvironment on HIF-1α-deficient MDSC, Gr-1⁺CD11b⁺ cells were isolated from spleens of tumor-bearing mice reconstituted with HIF-1α-deficient or WT BM and then injected directly into the ascites of CD45.1⁺ congenic mice. 12 h later, Gr-1⁺CD45.2⁺ donor MDSCs were isolated and used in experiments. MDSC with WT HIF-1α showed profound suppressive activity against T cells stimulated with anti-CD3/CD28 antibodies (Fig. 6 J). Expression of *arg1* and *inos* in HIF-1α-positive MDSC was dramatically up-regulated after transfer into the tumor site (Fig. 6 I). The suppressive effect of HIF-1α-deficient MDSC, as well as the expression of *arg1* and *inos* in these cells, was significantly ($P < 0.01$) lower (Fig. 6, I and J). Precisely the opposite effect was observed in the levels

of ROS. HIF-1 α -deficient MDSCs had substantially higher ROS production than their WT counterparts (Fig. 6 K).

In separate experiments, we evaluated the phenotype of donor cells in the tumor microenvironment by gating CD45.1⁺CD11b⁺ cells. The gating of CD11b⁺ cells was necessary to exclude CD45.2 EL-4 tumor cells from the analysis. Before transfer, the purity of Gr-1⁺CD11b⁺ cells was >95%. Within 24 h after the transfer of either WT or HIF-1 α -deficient MDSC, ~70% of donor (CD45.2⁺CD11b⁺) cells lost the expression of Gr-1 (unpublished data). Half of HIF-1 α WT Gr-1⁺ donor cells acquired the F4/80 marker of M Φ and 20% became CD11c⁺ DCs (Fig. 7 A). These results were similar to those described in Fig. 4 E demonstrating preferential differentiation of MDSC to M Φ in tumor microenvironment. In contrast, HIF-1 α -deficient MDSC acquired CD11c marker, with only 20% of cells expressing F4/80 (Fig. 7 A). As a result, the proportion of M Φ differentiated in tumor site from HIF-1 α WT MDSC was more than twofold higher than the proportion of cells differentiated from HIF-1 α -deficient MDSC ($P < 0.05$). Conversely, the proportion of CD11c⁺ DCs differentiated from HIF-1 α WT MDSC was more than threefold lower than that from HIF-1 α KO MDSC ($P < 0.01$; Fig. 7 A).

To verify the potential contribution of HIF-1 α to the effect of hypoxia on MDSC, HIF-1 α -deficient and WT MDSCs from spleens of tumor-bearing mice were cultured with GM-CSF for 5 d under hypoxic conditions. Hypoxia caused a dramatic up-regulation of *arg1* and *inos* in HIF-1 α WT MDSC, whereas a much smaller effect was observed in HIF-1 α -deficient MDSC (Fig. 7 B). Lack of HIF-1 α decreased the viability of cells. After a 5-d culture of MDSC, the number of recovered HIF-1 α -deficient cells was three times smaller than the number of HIF-1 α ^{+/+} cells. The proportion of cells that retained the MDSC phenotype among HIF-1 α ^{-/-} cells was slightly higher than among HIF-1 α ^{+/+} cells (Fig. 7 C). Consistent with our data described in Fig. 5, the vast majority of HIF-1 α WT MDSC differentiated into Gr-1⁺CD11b⁺F4/80 M Φ . In striking contrast, only a small proportion of HIF-1 α -deficient MDSC differentiated into M Φ (Fig. 7 C).

Next, we studied the possible effect of HIF-1 α on antitumor responses. BM cells from HIF-1 α KO or WT mice were transferred into lethally irradiated recipients, and 2 wk after the transfer mice were injected s.c. with B16.F10 tumor cells. When tumor became palpable (6 d after tumor inoculation), mice were injected with T cells from Pmel-1 transgenic mice.

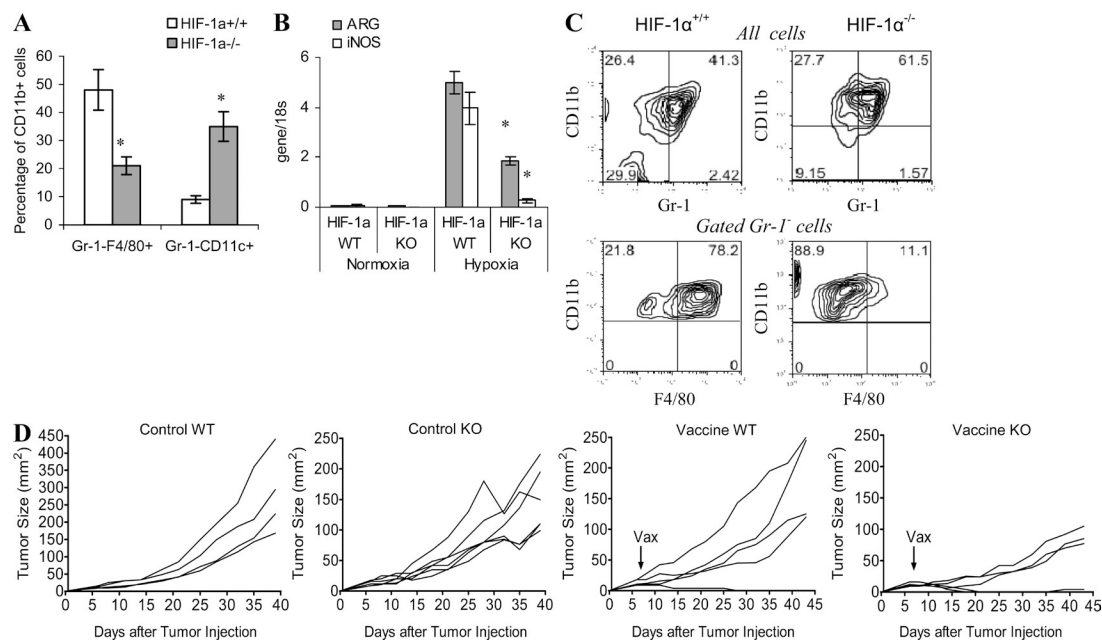


Figure 7. Changes in MDSC function and differentiation induced by the tumor-microenvironment require HIF-1 α . (A) Percentage of M Φ and DCs in the population of CD11b⁺Gr-1⁺CD45.2⁺ donor cells 18 h after the adoptive transfer of HIF-1 α ^{+/+} and HIF-1 α ^{-/-} MDSC into ascites tumors of congenic recipients. Each experiment included two mice per group and was performed twice. *, statistically significant ($P < 0.05$) differences between groups. (B and C) HIF-1 α -deficient and WT MDSCs were generated in vivo by transfer of BM cells into tumor-bearing recipients as described in A. MDSCs were isolated and cultured with GM-CSF for 5 d under hypoxic or normoxic conditions. Error bars show mean and SD. (B) Expression of *arg1* and *inos* was measured in triplicates in RT-PCR. Two independent experiments with the same results were performed. Error bars show mean and SD. (C) The phenotype of cells differentiated from MDSC after a 5-d culture with GM-CSF. Two independent experiments with the same results were performed. (D) Tumor growth of lethally irradiated mice reconstituted with either WT or HIF-1 α -deficient BM. Tumor was established by s.c. inoculation of 3×10^5 B16.F10 tumor cells 2 wk after transfer of BM to lethally irradiated recipients. Two groups of mice (control) were left untreated. Mice from two other groups received 3×10^6 splenocytes from Pmel-1 T cell receptor transgenic mice on day 6 after tumor inoculation. 1 d later, the mice were immunized with specific peptide. Tumor growth was monitored every 3–4 d in individually tagged mice by measuring two opposing diameters with a set of calipers. Each group included four to five mice. Results of individual mice are shown.

CD8⁺ T cells from these mice express TCR that recognizes D^b-restricted epitope corresponding to amino acid positions 25–33 of gp100 expressed in B16.F10 melanoma (Overwijk et al., 2003). Mice were immunized with specific peptide the next day. The control group included mice that did not receive T cells and immunization. This design allowed us to evaluate the antitumor effect of HIF-1 α WT antigen-specific T cells in the presence of WT or HIF-1 α -deficient myeloid cells that reconstitute BM during the first several weeks after the transfer. In both control groups, tumor grew progressively during first 4 wk. However, after that mice reconstituted with HIF-1 α -deficient BM demonstrated substantial delay in tumor growth ($P < 0.05$; Fig. 7 D). This effect could be explained by the reconstitution of lymphoid compartment by 7 wk after BM transfer. Adoptive transfer of T cells and immunization with specific peptide allowed for bypassing the need for lymphoid reconstitution. Immunization of WT mice delayed tumor progression in two out of five mice and, in one mouse, tumor was rejected (Fig. 7 D). This effect was substantially stronger in mice with HIF-1 α BM cells. Tumor was rejected in two mice and tumor growth was inhibited in the remaining three mice (Fig. 7 D).

DISCUSSION

In this study, we evaluated the nature of tumor-associated MDSC by comparing the phenotype and function of MDSC isolated from spleen and tumor sites from the same mice. It is known that MDSC can differentiate into M Φ and DC (Kusmartsev and Gabrilovich, 2003, 2005). Therefore, it was important to assure that we are indeed comparing cells with the same phenotype. We sorted MDSC based on the expression of Gr-1 and CD11b, two markers which are considered hallmarks of MDSC. MDSCs from the tumor site and spleen had similar morphology and phenotype. Expression of the macrophage cell marker F4/80 was slightly higher on tumor MDSC than on spleen cells. However, such rather minor phenotypic differences contrasted with profound differences in MDSC function. As was reported previously (Corzo et al., 2009), spleen MDSC contain a high level of ROS and a relatively modest level of NO and arginase I activity (although it was still elevated in comparison with Gr-1⁺CD11b⁺ cells from naive mice). In striking contrast, tumor MDSC had no increase in ROS over naive Gr-1⁺CD11b⁺ IMC but a very high level of NO and arginase I. These biochemical disparities translated into fundamental differences in their ability to suppress T cells. Tumor MDSCs were not only more potent inhibitors of antigen-specific T cell functions than spleen MDSCs but also, in contrast to spleen MDSCs, suppressed nonspecific T cells. Our experiments with a direct transfer of spleen MDSC to the tumor microenvironment demonstrated that 4 h was sufficient to cause dramatic changes in MDSC activity. These experiments also indicate that observed differences were indeed specific for the relative MDSC population and not caused by possible contamination of M Φ because the phenotype of MDSC was not changed within 4 h after transfer (unpublished data). Our recent study has found that in

spleens, granulocytic CD11b⁺Ly6G⁺Ly6C^{low} MDSCs produce a substantially higher level of ROS and a lower level of NO than monocytic CD11b⁺Ly6G⁺Ly6C^{high} cells (Youn et al., 2008). It was possible that the composition of these MDSC subsets could be different in spleens and tumors, which would explain the differences in functional activity of MDSC. However, the results of the experiments argue against this explanation.

Thus, this study demonstrated a dual role played by MDSC in immune suppression in cancer depending on their location. This may contribute to the phenomenon described previously in tumor-bearing mice. Although T cells from peripheral lymphoid organs of these mice did not respond to tumor-associated antigen, they nevertheless retained the ability to respond to nonspecific stimuli (Radoja et al., 2000; Yang and Lattime, 2003). Recent years have provided ample evidence supporting an important role of ROS in spleen MDSC-mediated suppression of T cells (Sinha et al., 2005; Kusmartsev et al., 2008; Markiewski et al., 2008; Youn et al., 2008; Mougiakakos et al., 2009). ROS was specifically implicated in antigen-specific T cell tolerance mediated by MDSC (Nagaraj et al., 2007; Hardy et al., 2008).

However, a very different situation is observed with T cells isolated directly from tumors. Tumor-infiltrating lymphocytes displayed a profound defect in their function that could be overcome only after culture of these cells in the presence of antigen-presenting cells and IL-2. One possible explanation of these differences could be that the tumor microenvironment contains a large number of different suppressive factors that are not present in spleens. Our data demonstrate that the tumor microenvironment can convert MDSCs into nonspecific suppressor cells by up-regulating proteins involved in the metabolism of L-arginine. These enzymes (iNOS and arginase I) are known to be actively involved in T cell suppression (Bronte and Zanovello, 2005; Rodríguez and Ochoa, 2008). Importantly, they do not require antigen-specific contact between MDSC and T cells to inhibit their function.

Up-regulation of *arg1* and *inos* by MDSC in the tumor site is a very rapid process and takes only several hours to occur. One of the major factors that distinguish the tumor microenvironment from lymphoid organs is hypoxia. It appears that hypoxia plays a critical role in the regulation of MDSC function by the tumor microenvironment. Our experiments have demonstrated that exposure of spleen MDSC to hypoxia could reproduce the effect of the tumor microenvironment on these cells by inducing a dramatic up-regulation of iNOS and *arg-1*, decreasing the expression of NOX2 and ROS and converting MDSC from antigen-specific to -nonspecific suppressors. How can hypoxia affect the function of MDSC? The major molecular mechanism of the hypoxia effect is mediated by the HIF-1 transcription factor. In hematopoietic cells, HIF-1 α is the predominant oxygen-sensitive subunit (Simon et al., 2002). Regulation of HIF-1 activity is mediated by posttranslational modification of the oxygen-dependent degradation (ODD) domain of HIF-1 α . At oxygen levels >5%, hydroxylation of the proline residues 402 and 564 in the

ODD of HIF-1 α enables binding of the ubiquitination ligase von Hippel-Lindau tumor suppressor protein, which leads to degradation of HIF-1 α by the proteasome. In contrast, at oxygen levels <5%, hydroxylation is inhibited leading to stabilization of HIF-1 α . HIF-1 α has been directly implicated in the up-regulation of *iNOS* (for review see Yang et al., 2002) and *arginase* (Albina and Reichner, 2003; Sica and Bronte, 2007) in macrophages. HIF-1 α has been shown to suppress oxidative phosphorylation and ROS production in mitochondria (Kim et al., 2006; Papandreou et al., 2006). Our data demonstrated that HIF-1 α is directly responsible for conversion of MDSC in the tumor microenvironment to antigen-nonspecific suppressors of T cell function via up-regulation of *arginase* and NO.

Our data also indicate that hypoxia, primarily via HIF-1 α , has a direct effect on MDSC differentiation. 2 d after adoptive transfer, >60% of MDSC in the spleen retained an immature phenotype, whereas the rest of the cells differentiated evenly into M Φ and DCs. In contrast, MDSC transferred into tumor site differentiated much more rapidly, with most of the cells acquiring the phenotype of M Φ . Experiments with MDSC culture in hypoxic conditions recapitulated these findings. Stabilization of HIF-1 α with DFO reproduced this effect, suggesting that HIF-1 α could be an important factor regulating the differentiation of MDSC to TAM. MDSC lacking HIF-1 α did not differentiate into TAM within the tumor microenvironment or hypoxia but instead acquired markers of DCs.

Experiments with vaccination of HIF-1 α -deficient tumor-bearing mice support an important role of HIF-1 α in anti-tumor responses. Even without vaccination, mice that received HIF-1 α -deficient BM cells demonstrated a significant delay in tumor progression. This effect was observed only 4–5 wk after tumor inoculation and could be possibly explained by the reconstitution of the lymphoid compartment by that time (6–7 wk after BM transfer). Stronger antitumor responses were not necessarily the result of improved function of myeloid cells because HIF-1 α is known to negatively affect the function of T cells as well. Deletion of HIF-1 α in T cells resulted in their activation in vitro and in vivo (Lukashev et al., 2006; Thiel et al., 2007). However, experiments with adoptive transfer of antigen-specific Pmel-1 T cells (which are HIF-1 α ^{+/+}) and vaccination of mice 1 wk after tumor inoculation allowed for better interpretation of the results. Our experiments indicated that mice that received HIF-1 α -deficient BM developed stronger antitumor response than mice with WT HIF-1 α BM. It is important to point out that those experiments, although suggestive, cannot definitively address the specific effect of HIF-1 α deletion in MDSC because lack of HIF-1 α in other myeloid cells (DC and M Φ) may also impact antitumor responses. More specific depletion experiments will be necessary to clarify this question.

Our study may suggest a model of MDSC differentiation and function in cancer. Expansion of IMCs in BM of tumor-bearing hosts, which is governed in large part by up-regulation of STAT3 (Nefedova et al., 2004; Cheng et al., 2008; Kujawski et al., 2008), results in an accumulation of MDSC in

peripheral lymphoid organs and in the tumor site. In lymphoid organs, MDSCs retain a high level of NOX2 and increased ROS levels. This is associated with a little increase in NO production and *arginase* I activity. As a result, these MDSCs produce peroxynitrite and exert their effect only via close cell–cell contact with activated antigen-specific T cells, which induce antigen-specific T cell tolerance. At the same time, these MDSCs fail to suppress antigen-nonspecific activation of T cells. In contrast, at the tumor site, MDSCs, as a result of the effect of hypoxia via HIF-1 α , dramatically up-regulate expression of *inos* and *argI*, which is associated with down-regulation of both NOX2 expression and ROS production. Because of these changes, MDSCs acquire the ability to suppress antigen-nonspecific T cell functions, which contribute to the profound immune suppression observed within the tumor microenvironment. In addition, hypoxia via HIF-1 α promotes differentiation of MDSC to immune suppressive TAM, which further supports the immune-suppressive network (Fig. S8). Elucidation of this dual role of MDSC may not only help to understand the biology of tumor-associated immune suppression but also suggest that any therapeutic interventions should take into account the effect of microenvironment on the function of these cells.

MATERIALS AND METHODS

Mice and tumor models

All experiments with mice were approved by University of South Florida Animal Care and Use Committee. C57BL/6 and BALB/c female mice (6–8 wk of age) were obtained from the National Cancer Institute. Mice were kept in pathogen-free conditions. CD45.1⁺ congenic mice (B6.SJL-PtcrPep3b/BoyJ), gp91^{phox}^{-/-} (B6.129S6-Cybbtm1Din), HIF-1 α ^{flax/flax} (B6.129-Hif1atm3Rsj/JE), and Mx1-Cre^{+/+} (C57BL/6J-Tg(Mx1-cre)1Cgn/J) were purchased from The Jackson Laboratory. 2C TCR transgenic mice have been described previously (Nagaraj et al., 2007). EL4 thymoma was obtained from American Type Culture Collection. To establish s.c. tumors, 5 × 10⁵ EL-4 tumor cells were injected into C57BL/6 mice. This number of cells formed a tumor with a 1.5-cm diameter within 2–3 wk of injection. EL-4 ascitic tumor was generated by injecting 3 × 10⁵ tumor cells i.p. into C57BL/6 mice. To harvest cells from ascitic tumors, mice were sacrificed and the peritoneum was washed with 10 ml of ice-cold PBS. Cells were then aspirated and placed on ice immediately. The CT26 colon carcinoma model used in some in vitro experiments was established by injecting 5 × 10⁵ CT26 tumor cells s.c. into BALB/c mice. The *mCC10TAg* transgene model of lung cancer was described previously (Magdaleno et al., 1997).

Patients

14 patients (47–78 yr old) with resectable T3 or T4 and N2b stage of HNC were enrolled in the study after signing University of South Florida IRB-approved consent. Patients did not receive radiation or chemotherapy for at least 3 mo before sample collection. Peripheral blood and tumor tissues were collected at the time of surgery from all patients. To obtain single cell suspensions from tumors, solid tissue was subjected to 1 h of enzymatic digestion using 0.1 mg/ml hyaluronidase (Sigma-Aldrich), 2 mg/ml collagenase (Sigma-Aldrich), 600 U/ml DNase (Sigma-Aldrich), and 0.2 mg/ml protease (Sigma-Aldrich) in RPMI 1640. The digested tissue was passed through a 70- μ m mesh, and erythrocytes were removed by hypotonic lysis and washed thoroughly to remove debris. Mononuclear cell suspensions were obtained from whole blood using density gradient centrifugation. All cell samples were analyzed within 3 h after collection. Cells were loaded with DCFDA. To identify live MDSC, mononuclear cells were first labeled with PerCP-Cy5.5-conjugated anti-CD14, APC-conjugated anti-CD11b, and PE-Cy7-conjugated anti-CD33. Antibody-labeled cells were then finally resuspended in DAPI buffer to identify viable cells before data collection.

To detect iNOS in MDSCs after surface staining with PerCP-Cy5.5-conjugated anti-CD14, APC-conjugated anti-CD11b and PE-Cy-7-conjugated anti-CD33 antibodies were fixed, permeabilized using the Cytotfix/Cytoperm Fixation/Permeabilization kit (BD), and analyzed using an LSR II flow cytometer (BD). At least 100,000 cells were collected for each parameter to obtain reliable data. Analysis of the samples was performed essentially as described elsewhere (Mirza et al., 2006).

Cell isolation

To collect splenocytes, single cell suspensions were prepared from spleens, and red cells were removed using ammonium chloride lysis buffer. MDSCs were isolated by cell sorting on a FACS Aria (BD) after cell staining with APC-conjugated anti-Gr-1 antibody and PE-conjugated anti-CD11b antibodies. To harvest peritoneal macrophages, mice were injected i.p. with 1 ml thioglycollate (BD). 3 d later, peritoneal cells were obtained by peritoneal lavage with 10 ml of ice-cold PBS. Peritoneal macrophages were harvested using magnetic beads and biotinylated anti-F4/80 antibody.

Reagents

Arginase inhibitor NW-hydroxyl-nor-L-arginine (nor-NOHA) and iNOS inhibitor NG-monomethyl-L-arginine (L-NMMA) were obtained from EMD. 2C-specific (H-2K^b, SIYRYYYGL) and control (H-2K^b RAHYNIVTF) peptides were obtained from American Peptide Company. DCFDA was purchased from Invitrogen. Antibodies against p47^{phox} were purchased from Santa Cruz Biotechnology, Inc., anti-HIF-1 α antibody from R&D Systems, and biotinylated anti-F4/80 antibody from AbD Serotec. All other antibodies used for flow cytometry were purchased from BD.

MDSC isolation from solid tumors

Tumors were dissected and digested with 0.7 mg/ml collagenase XI (Sigma-Aldrich) and 30 mg/ml of type IV bovine pancreatic DNase (Sigma-Aldrich) for 45 min at 37°C. Remaining red cells were lysed by ACK and dead cells were removed by centrifugation with Lympholyte M. Gr-1⁺ cells were isolated by using biotinylated anti-Gr-1 antibody and streptavidin microbeads with MiniMACS columns (Miltenyi Biotec).

Cell culture and hypoxic conditions

MDSCs were cultured in complete RPMI media containing 10 ng/ml GM-CSF. A hypoxic environment (1% O₂ with 5% CO₂) was created and maintained using a C-Chamber Hypoxic Incubator Chamber (BioSpherix).

ROS detection, arginase activity and NO production

The oxidation-sensitive dye DCFDA was used to measure ROS production by MDSC. Cells were incubated at 37°C in RPMI in the presence of 2.5 μ M DCFDA for 30 min. For PMA-induced activation, cells were simultaneously cultured, along with DCFDA, with 30 ng/ml PMA (Sigma-Aldrich). Cells were then labeled with anti-Gr-1 and anti-CD11b antibodies on ice and evaluated by flow cytometry.

Arginase activity was measured in cell lysates, as previously described (Kusmartsev and Gabrilovich, 2005). In brief, cells were lysed for 30 min with 0.1% Triton X-100. To 100 μ l of protein lysate (25 μ g/ml), 100 μ l of 25 mM Tris-HCl and 10 μ l of 10 mM MnCl₂ were added, and the enzyme was activated by heating for 10 min at 56°C. Arginine hydrolysis was conducted by incubating the lysate with 100 μ l of 0.5 M L-arginine, pH 9.7, at 37°C for 120 min. The reaction was stopped with 900 μ l H₂SO₄ (96%)/H₃PO₄ (85%)/H₂O (1/3/7, vol/vol/vol). The urea concentration was measured at 540 nm after addition of 40 μ l β -isonitrosopropiophenone (dissolved in 100% ethanol), followed by heating at 95°C for 30 min. One unit of enzyme activity is defined as the amount of enzyme that catalyzed the formation of 1 μ mol urea per min.

To detect nitrites, equal volumes of culture supernatants (100 μ l) were mixed with Greiss reagent. After a 10-min incubation at room temperature, the absorbance at 550 nm was measured using a microplate plate reader (Bio-Rad Laboratories). Nitrite concentrations were determined by comparing the absorbance values for the test samples to a standard curve generated by serial dilution of 0.25 mM sodium nitrite.

qRT-PCR

RNA was extracted with Trizol (Invitrogen). cDNA was synthesized and used for the evaluation of gene expression as described previously (Nefedova et al., 2007). To detect *arg1*, *inos*, *gp91^{phox}*, and *p47^{phox}*, PCR was performed with 2 μ l cDNA, TaqMan Universal PCR Master Mix (Applied Biosystems), and target gene assay mix containing sequence-specific primers and 6-carboxyfluorescein dye-labeled TaqMan minor groove binder probe (Applied Biosystems). Amplification with 18S endogenous control assay mix was used for controls. PCR was performed in triplicate for each sample. Data quantitation was performed using the relative standard curve method. Expression levels of the genes were normalized by 18S mRNA. To detect expression of cytokines and β -actin, PCR was performed with 12.5 μ l SYBR Master Mixture (Applied Biosystems) and the following primers: sense⁺ IL-6, 5'-ATCCAGTTGCCTTCTTGGG-ACTGA-3'; IL-12, 5'-ATGCAGCAAGTGGGCATGTGTT-3'; TGF- β , 5'-TACGTCAGACATTCCGGGAAGCAGT-3'; IL-10, 5'-TACCAAA-GCCACAAAGCAGCCT-3'; and β -actin, 5'-ACCGCTCGTTGCCAATA-GTGATGA-3'. The expression of IL-6, TGF- β , IL-12, and IL-10 were normalized to β -actin.

Western blotting

Cells were lysed in TNE buffer (20 mM Tris-HCl, pH 7.5, 150 mM NaCl, and 1 mM EDTA) containing 1% NP-40 in the presence of protease and phosphatase inhibitors. Whole-cell lysates were subjected to 8% SDS-PAGE and transferred to PVDF membranes. Membranes were probed with appropriate primary antibodies overnight at 4°C. Membranes were washed and incubated overnight at 4°C with secondary antibody conjugated with peroxidase. Results were visualized by chemiluminescence detection using a commercial kit (GE Healthcare). To confirm equal loading, membranes were stripped and reprobed with antibody against β -actin (Santa Cruz Biotechnology, Inc.).

Evaluation of T cell function

Proliferation. Splenocytes from 2C transgenic mice, depleted of red cells, were placed in triplicates into U-bottom 96-well plates (2 \times 10⁵/well). For antigen-specific responses, splenocytes were cultured in the presence of cognate antigen (2C-specific peptide SIYRYYYGL) and cultured for 72 h. For anti-CD3/CD28 antibody-induced T cell proliferation, splenocytes were cultured in the presence of 1 μ g/ml anti-CD3 antibody and 5 μ g/ml anti-CD28 antibody. 18 h before harvesting, cells were pulsed with ³H-thymidine (1 μ Ci/well; GE Healthcare). ³H-thymidine uptake was counted using a liquid scintillation counter and expressed as cpm.

IFN- γ production. The number of IFN- γ -producing cells in response to cognate antigens or CD3/CD28 antibodies were evaluated in an ELISPOT assay as previously described (Nagaraj et al., 2007). Each well contained 10⁵ splenocytes. The number of spots was counted in triplicates and calculated by an automatic ELISPOT counter (Cellular Technology).

Treatment of tumor-bearing mice

Mice were inoculated s.c. with 3 \times 10⁵ B16 tumor cells, and 6 d later the mice received 3 \times 10⁶ splenocytes from Pmel-1 T cell receptor transgenic mice. 1 d later, the mice were immunized with 200 μ g Hg₁₀₀₂₅₋₃₃ peptide (KVPRNQDWL) mixed with 2 toll-like receptor agonists (50 μ g poly-IC and 100 μ g CpG-1826). Poly-IC (Hiltonol, a clinical grade stabilized formulation containing poly-L-lysine and carboxymethyl cellulose) was provided by A. Salazar (Oncovir, Inc., Washington, DC). CpG-1826 was prepared by the Mayo Clinic Molecular Core Facility. Tumor growth was monitored every 3–4 d in individually tagged mice by measuring two opposing diameters with a set of calipers.

Evaluation of the presence of myeloid cells in the areas of hypoxia in tumor

To detect hypoxia, we used pimonidazole HCl, which is activated in hypoxic cells and forms stable covalent adducts with thiol groups in proteins, peptides, and amino acids. The antibody reagent binds to these adducts, allowing

their detection by immunochemical means. 60 mg/kg pimonidazole HCl (Hypoxyprobe) was injected i.v. into EL4 tumor-bearing mice. 30 min later, tumor tissues were collected and processed for immunohistochemical staining with MA1 against hypoxia and anti-Gr1 or anti-F4/80 antibodies (BD). The secondary biotinylated antibodies and the color development systems VECTASTAIN ABC kits and substrate kits (Vector Laboratories) were used for detection.

Statistics

Statistical analysis was performed using a two-tailed Mann-Whitney *U* or Wilcoxon nonparametric test and Prism 5 software (GraphPad Software, Inc.), with significance determined at $P < 0.05$.

Online supplemental material

Fig. S1 shows the effect of MDSC isolated from spleens and tumors of CC10 transgenic mice on T cell proliferation. Fig. S2 shows iNOS in MDSC from tumor and spleens of EL-4 tumor-bearing mice. Fig. S3 shows ROS in MDSC from tumor and spleens of EL-4 tumor-bearing mice. Fig. S4 shows the effect of the tumor microenvironment on MDSC function after adoptive transfer. Fig. S5 shows a typical example of MDSC differentiation in tumor site and spleens of EL-4 tumor-bearing mice. Fig. S6 shows the effect of hypoxia on the phenotype of MDSC. Fig. S7 shows the effect of hypoxia on differentiation of MΦ with M1 and M2 phenotypes. Fig. S8 shows a schematic of MDSC function and differentiation in tumor-bearing host. Online supplemental material is available at <http://www.jem.org/cgi/content/full/jem.20100587/DC1>.

We thank N. Olashaw for assistance in preparation of the manuscript.

This work was supported by National Institutes of Health (NIH) grant CA 84488 to D.I. Gabrilovich, NIH F31 fellowship to C.A. Corzo, and NIH grants R01CA103921 and R01CA136828 to E. Celis. This work has been supported in part by the Analytic Microscopy and Flow Cytometry Core Facility at the H. Lee Moffitt Cancer Center.

Authors declare no competing financial interests.

Submitted: 24 March 2010

Accepted: 31 August 2010

REFERENCES

- Albina, J.E., and J.S. Reichner. 2003. Oxygen and the regulation of gene expression in wounds. *Wound Repair Regen.* 11:445–451. doi:10.1046/j.1524-475X.2003.11619.x
- Almand, B., J.I. Clark, E. Nikitina, J. van Beynen, N.R. English, S.C. Knight, D.P. Carbone, and D.I. Gabrilovich. 2001. Increased production of immature myeloid cells in cancer patients: a mechanism of immunosuppression in cancer. *J. Immunol.* 166:678–689.
- Bronte, V., and P. Zanovello. 2005. Regulation of immune responses by L-arginine metabolism. *Nat. Rev. Immunol.* 5:641–654. doi:10.1038/nri1668
- Cheng, P., C.A. Corzo, N. Luetke, B. Yu, S. Nagaraj, M.M. Bui, M. Ortiz, W. Nacken, C. Sorg, T. Vogl, et al. 2008. Inhibition of dendritic cell differentiation and accumulation of myeloid-derived suppressor cells in cancer is regulated by S100A9 protein. *J. Exp. Med.* 205:2235–2249. doi:10.1084/jem.20080132
- Corzo, C.A., M.J. Cotter, P. Cheng, S. Kusmartsev, E. Sotomayor, T. Padhya, T.V. McCaffrey, J.C. McCaffrey, and D.I. Gabrilovich. 2009. Mechanism regulating reactive oxygen species in tumor-induced myeloid-derived suppressor cells. *J. Immunol.* 182:5693–5701. doi:10.4049/jimmunol.0900092
- Diaz-Montero, C.M., M.L. Salem, M.I. Nishimura, E. Garrett-Mayer, D.J. Cole, and A.J. Montero. 2009. Increased circulating myeloid-derived suppressor cells correlate with clinical cancer stage, metastatic tumor burden, and doxorubicin-cyclophosphamide chemotherapy. *Cancer Immunol. Immunother.* 58:49–59. doi:10.1007/s00262-008-0523-4
- Fricke, I., N. Mirza, J. Dupont, C. Lockhart, A. Jackson, J.-H. Lee, J.A. Sosman, and D.I. Gabrilovich. 2007. Vascular endothelial growth factor-trap overcomes defects in dendritic cell differentiation but does not improve antigen-specific immune responses. *Clin. Cancer Res.* 13:4840–4848. doi:10.1158/1078-0432.CCR-07-0409
- Gabrilovich, D.I., and S. Nagaraj. 2009. Myeloid-derived suppressor cells as regulators of the immune system. *Nat. Rev. Immunol.* 9:162–174. doi:10.1038/nri2506
- Hardy, L.L., D.A. Wick, and J.R. Webb. 2008. Conversion of tyrosine to the inflammation-associated analog 3'-nitrotyrosine at either TCR- or MHC-contact positions can profoundly affect recognition of the MHC class I-restricted epitope of lymphocytic choriomeningitis virus glycoprotein 33 by CD8 T cells. *J. Immunol.* 180:5956–5962.
- Kim, J.W., I. Tchernyshyov, G.L. Semenza, and C.V. Dang. 2006. HIF-1-mediated expression of pyruvate dehydrogenase kinase: a metabolic switch required for cellular adaptation to hypoxia. *Cell Metab.* 3:177–185. doi:10.1016/j.cmet.2006.02.002
- Kujawski, M., M. Kortylewski, H. Lee, A. Herrmann, H. Kay, and H. Yu. 2008. Stat3 mediates myeloid cell-dependent tumor angiogenesis in mice. *J. Clin. Invest.* 118:3367–3377. doi:10.1172/JCI35213
- Kusmartsev, S., and D.I. Gabrilovich. 2003. Inhibition of myeloid cell differentiation in cancer: the role of reactive oxygen species. *J. Leukoc. Biol.* 74:186–196. doi:10.1189/jlb.0103010
- Kusmartsev, S., and D.I. Gabrilovich. 2005. STAT1 signaling regulates tumor-associated macrophage-mediated T cell deletion. *J. Immunol.* 174:4880–4891.
- Kusmartsev, S., and D.I. Gabrilovich. 2006. Role of immature myeloid cells in mechanisms of immune evasion in cancer. *Cancer Immunol. Immunother.* 55:237–245. doi:10.1007/s00262-005-0048-z
- Kusmartsev, S., Y. Nefedova, D. Yoder, and D.I. Gabrilovich. 2004. Antigen-specific inhibition of CD8+ T cell response by immature myeloid cells in cancer is mediated by reactive oxygen species. *J. Immunol.* 172:989–999.
- Kusmartsev, S., S. Nagaraj, and D.I. Gabrilovich. 2005. Tumor-associated CD8+ T cell tolerance induced by bone marrow-derived immature myeloid cells. *J. Immunol.* 175:4583–4592.
- Kusmartsev, S., Z. Su, A. Heiser, J. Dannull, E. Eruslanov, H. Kübler, D. Yancey, P. Dahm, and J. Vieweg. 2008. Reversal of myeloid cell-mediated immunosuppression in patients with metastatic renal cell carcinoma. *Clin. Cancer Res.* 14:8270–8278. doi:10.1158/1078-0432.CCR-08-0165
- Lewis, C., and C. Murdoch. 2005. Macrophage responses to hypoxia: implications for tumor progression and anti-cancer therapies. *Am. J. Pathol.* 167:627–635.
- Lopez, C.B., T.D. Rao, H. Feiner, R. Shapiro, J.R. Marks, and A.B. Frey. 1998. Repression of interleukin-2 mRNA translation in primary human breast carcinoma tumor-infiltrating lymphocytes. *Cell. Immunol.* 190:141–155. doi:10.1006/cimm.1998.1390
- Lukashev, D., B. Klebanov, H. Kojima, A. Grinberg, A. Ohta, L. Berenfeld, R.H. Wenger, A. Ohta, and M. Sitkovsky. 2006. Cutting edge: hypoxia-inducible factor 1α and its activation-inducible short isoform I.1 negatively regulate functions of CD4+ and CD8+ T lymphocytes. *J. Immunol.* 177:4962–4965.
- Magdaleno, S.M., G. Wang, V.L. Mireles, M.K. Ray, M.J. Finegold, and F.J. DeMayo. 1997. Cyclin-dependent kinase inhibitor expression in pulmonary Clara cells transformed with SV40 large T antigen in transgenic mice. *Cell Growth Differ.* 8:145–155.
- Markiewski, M.M., R.A. DeAngelis, F. Benencia, S.K. Ricklin-Lichtsteiner, A. Koutoulaki, C. Gerard, G. Coukos, and J.D. Lambris. 2008. Modulation of the antitumor immune response by complement. *Nat. Immunol.* 9:1225–1235. doi:10.1038/ni.1655
- Mirza, N., M. Fishman, I. Fricke, M. Dunn, A.M. Neuger, T.J. Frost, R.M. Lush, S. Antonia, and D.I. Gabrilovich. 2006. All-trans-retinoic acid improves differentiation of myeloid cells and immune response in cancer patients. *Cancer Res.* 66:9299–9307. doi:10.1158/0008-5472.CAN-06-1690
- Monu, N., and A.B. Frey. 2007. Suppression of proximal T cell receptor signaling and lytic function in CD8+ tumor-infiltrating T cells. *Cancer Res.* 67:11447–11454. doi:10.1158/0008-5472.CAN-07-1441
- Mougiakakos, D., C.C. Johansson, and R. Kiessling. 2009. Naturally occurring regulatory T cells show reduced sensitivity toward oxidative stress-induced cell death. *Blood.* 113:3542–3545. doi:10.1182/blood-2008-09-181040
- Movahedi, K., M. Guillems, J. Van den Bossche, R. Van den Bergh, C. Gysemans, A. Beschinn, P. De Baetselier, and J.A. Van Ginderachter.

2008. Identification of discrete tumor-induced myeloid-derived suppressor cell subpopulations with distinct T cell-suppressive activity. *Blood*. 111:4233–4244. doi:10.1182/blood-2007-07-099226
- Movahedi, K., D. Laoui, C. Gysemans, M. Baeten, G. Stangé, J. Van den Bossche, M. Mack, D. Pipeleers, P. In't Veld, P. De Baetselier, and J.A. Van Ginderachter. 2010. Different tumor microenvironments contain functionally distinct subsets of macrophages derived from Ly6C(high) monocytes. *Cancer Res.* 70:5728–5739. doi:10.1158/0008-5472.CAN-09-4672
- Nagaraj, S., K. Gupta, V. Pisarev, L. Kinarsky, S. Sherman, L. Kang, D.L. Herber, J. Schneck, and D.I. Gabrilovich. 2007. Altered recognition of antigen is a mechanism of CD8⁺ T cell tolerance in cancer. *Nat. Med.* 13:828–835. doi:10.1038/nm1609
- Nagaraj, S., J.I. Youn, H. Weber, C. Iclozan, L. Lu, M.J. Cotter, C. Meyer, C.R. Becerra, M. Fishman, S. Antonia, et al. 2010. Anti-inflammatory triterpenoid blocks immune suppressive function of MDSCs and improves immune response in cancer. *Clin. Cancer Res.* 16:1812–1823. doi:10.1158/1078-0432.CCR-09-3272
- Nefedova, Y., M. Huang, S. Kusmartsev, R. Bhattacharya, P. Cheng, R. Salup, R. Jove, and D. Gabrilovich. 2004. Hyperactivation of STAT3 is involved in abnormal differentiation of dendritic cells in cancer. *J. Immunol.* 172:464–474.
- Nefedova, Y., M. Fishman, S. Sherman, X. Wang, A.A. Beg, and D.I. Gabrilovich. 2007. Mechanism of all-trans retinoic acid effect on tumor-associated myeloid-derived suppressor cells. *Cancer Res.* 67:11021–11028. doi:10.1158/0008-5472.CAN-07-2593
- Ostrand-Rosenberg, S., and P. Sinha. 2009. Myeloid-derived suppressor cells: linking inflammation and cancer. *J. Immunol.* 182:4499–4506. doi:10.4049/jimmunol.0802740
- Overwijk, W.W., M.R. Theoret, S.E. Finkelstein, D.R. Surman, L.A. de Jong, F.A. Vyth-Dreese, T.A. Dellemijn, P.A. Antony, P.J. Spiess, D.C. Palmer, et al. 2003. Tumor regression and autoimmunity after reversal of a functionally tolerant state of self-reactive CD8⁺ T cells. *J. Exp. Med.* 198:569–580. doi:10.1084/jem.20030590
- Pan, P.Y., G. Ma, K.J. Weber, J. Ozao-Choy, G. Wang, B. Yin, C.M. Divino, and S.H. Chen. 2010. Immune stimulatory receptor CD40 is required for T-cell suppression and T regulatory cell activation mediated by myeloid-derived suppressor cells in cancer. *Cancer Res.* 70:99–108. doi:10.1158/0008-5472.CAN-09-1882
- Papandreou, I., R.A. Cairns, L. Fontana, A.L. Lim, and N.C. Denko. 2006. HIF-1 mediates adaptation to hypoxia by actively downregulating mitochondrial oxygen consumption. *Cell Metab.* 3:187–197. doi:10.1016/j.cmet.2006.01.012
- Peranzoni, E., S. Zilio, I. Marigo, L. Dolcetti, P. Zanovello, S. Mandruzzato, and V. Bronte. 2010. Myeloid-derived suppressor cell heterogeneity and subset definition. *Curr. Opin. Immunol.* 22:238–244. doi:10.1016/j.coi.2010.01.021
- Rabinovich, G.A., D. Gabrilovich, and E.M. Sotomayor. 2007. Immunosuppressive strategies that are mediated by tumor cells. *Annu. Rev. Immunol.* 25:267–296. doi:10.1146/annurev.immunol.25.022106.141609
- Rabinovich, H., M. Banks, T.E. Reichert, T.F. Logan, J.M. Kirkwood, and T.L. Whiteside. 1996. Expression and activity of signaling molecules in T lymphocytes obtained from patients with metastatic melanoma before and after interleukin 2 therapy. *Clin. Cancer Res.* 2:1263–1274.
- Radoja, S., T.D. Rao, D. Hillman, and A.B. Frey. 2000. Mice bearing late-stage tumors have normal functional systemic T cell responses in vitro and in vivo. *J. Immunol.* 164:2619–2628.
- Reichert, T.E., L. Strauss, E.M. Wagner, W. Gooding, and T.L. Whiteside. 2002. Signaling abnormalities, apoptosis, and reduced proliferation of circulating and tumor-infiltrating lymphocytes in patients with oral carcinoma. *Clin. Cancer Res.* 8:3137–3145.
- Rodríguez, P.C., and A.C. Ochoa. 2008. Arginine regulation by myeloid derived suppressor cells and tolerance in cancer: mechanisms and therapeutic perspectives. *Immunol. Rev.* 222:180–191. doi:10.1111/j.1600-065X.2008.00608.x
- Sica, A., and V. Bronte. 2007. Altered macrophage differentiation and immune dysfunction in tumor development. *J. Clin. Invest.* 117:1155–1166. doi:10.1172/JCI31422
- Simon, M.C., D. Ramirez-Bergeron, F. Mack, C.J. Hu, Y. Pan, and K. Mansfield. 2002. Hypoxia, HIFs, and cardiovascular development. *Cold Spring Harb. Symp. Quant. Biol.* 67:127–132. doi:10.1101/sqb.2002.67.127
- Sinha, P., V.K. Clements, and S. Ostrand-Rosenberg. 2005. Reduction of myeloid-derived suppressor cells and induction of M1 macrophages facilitate the rejection of established metastatic disease. *J. Immunol.* 174:636–645.
- Srivastava, M.K., P. Sinha, V.K. Clements, P. Rodriguez, and S. Ostrand-Rosenberg. 2010. Myeloid-derived suppressor cells inhibit T-cell activation by depleting cystine and cysteine. *Cancer Res.* 70:68–77. doi:10.1158/0008-5472.CAN-09-2587
- Talmadge, J.E. 2007. Pathways mediating the expansion and immunosuppressive activity of myeloid-derived suppressor cells and their relevance to cancer therapy. *Clin. Cancer Res.* 13:5243–5248. doi:10.1158/1078-0432.CCR-07-0182
- Thiel, M., C.C. Caldwell, S. Kreth, S. Kuboki, P. Chen, P. Smith, A. Ohta, A.B. Lentsch, D. Lukashev, and M.V. Sitkovsky. 2007. Targeted deletion of HIF-1 α gene in T cells prevents their inhibition in hypoxic inflamed tissues and improves septic mice survival. *PLoS One*. 2:e853. doi:10.1371/journal.pone.0000853
- Yamamoto, Y., H. Ishigaki, H. Ishida, Y. Itoh, Y. Noda, and K. Ogasawara. 2008. Analysis of splenic Gr-1^{int} immature myeloid cells in tumor-bearing mice. *Microbiol. Immunol.* 52:47–53. doi:10.1111/j.1348-0421.2008.00009.x
- Yang, A.S., and E.C. Lattime. 2003. Tumor-induced interleukin 10 suppresses the ability of splenic dendritic cells to stimulate CD4 and CD8 T-cell responses. *Cancer Res.* 63:2150–2157.
- Yang, D.I., J.H. Yin, S. Mishra, R. Mishra, and C.Y. Hsu. 2002. NO-mediated chemoresistance in C6 glioma cells. *Ann. N. Y. Acad. Sci.* 962:8–17. doi:10.1111/j.1749-6632.2002.tb04052.x
- Youn, J.I., S. Nagaraj, M. Collazo, and D.I. Gabrilovich. 2008. Subsets of myeloid-derived suppressor cells in tumor-bearing mice. *J. Immunol.* 181:5791–5802.
- Zea, A.H., P.C. Rodriguez, M.B. Atkins, C. Hernandez, S. Signoretti, J. Zabaleta, D. McDermott, D. Quiceno, A. Youmans, A. O'Neill, et al. 2005. Arginase-producing myeloid suppressor cells in renal cell carcinoma patients: a mechanism of tumor evasion. *Cancer Res.* 65:3044–3048.
- Zhou, R., P.L. He, Y.X. Ren, W.H. Wang, R.Y. Zhou, H. Wan, S. Ono, H. Fujiwara, and J.P. Zuo. 2007. Myeloid suppressor cell-associated immune dysfunction in CSA1M fibrosarcoma tumor-bearing mice. *Cancer Sci.* 98:882–889. doi:10.1111/j.1349-7006.2007.00465.x